Published October 17, 2011

DOCK8 deficiency impairs CD8 T cell survival and function in humans and mice

Katrina L. Randall,[1,2] Stephanie S.-Y. Chan,[1] Cindy S. Ma,[3,4] Ivan Fung,[5,6] Yan Mei,[1] Mehmet Yabas,[1] Andy Tan,[1] Peter D. Arkwright,[7] Wafaa Al Suwairi,[8] Saul Oswaldo Lugo Reyes,[9] Marco A. Yamazaki-Nakashimada,[10] Maria de la Luz Garcia-Cruz,[11] Joanne M. Smart,[12] Capucine Picard,[13,14,15] Satoshi Okada,[16] Emmanuelle Jouanguy,[14,15,16] Jean-Laurent Casanova,[14,15,16] Teresa Lambe,[17] Richard J. Cornall,[17] Sarah Russell,[5,6,18] Jane Oliaro,[5,6] Stuart G. Tangye,[3,4] Edward M. Bertram,[1] and Christopher C. Goodnow[1]

[1]Department of Immunology, The John Curtin School of Medical Research and [2]Australian National University Medical School, Australian National University, Canberra, Australian Capital Territory 0200, Australia
[3]Immunology Program, Garvan Institute of Medical Research, Darlinghurst, Sydney, New South Wales 2010, Australia
[4]St. Vincent's Clinical School, Faculty of Medicine, University of New South Wales, Kensington, New South Wales 2052, Australia
[5]Cancer Immunology Division, Peter MacCallum Cancer Centre, East Melbourne, Victoria 3002, Australia
[6]Department of Pathology, The University of Melbourne, Parkville, Victoria 3010, Australia
[7]Royal Manchester Children's Hospital, The University of Manchester, Manchester M13 9WL, England, UK
[8]King Abdullah International Medical Research Center, King Abdul-Aziz Medical Center, Riyadh 11426, Saudi Arabia
[9]Immunodeficiencies Research Unit and [10]Clinical Immunology Department, National Institute of Pediatrics, Mexico City 04530, Mexico
[11]Allergy and Clinical Immunology Department, National Institute of Respiratory Diseases, Mexico City 14080, Mexico
[12]Allergy and Immunology Department, Royal Children's Hospital, Parkville, Victoria 3052, Australia
[13]Study Center of Primary Immunodeficiencies, Necker Hospital, 75015 Paris, France
[14]Necker Medicine Faculty, Sorbonne Paris Cité, Paris Descartes University, 75015 Paris, France
[15]Laboratory of Human Genetics of Infectious Diseases, Necker Branch, National Institute of Health and Medical Research, U980, 75015 Paris, France
[16]St. Giles Laboratory of Human Genetics of Infectious Diseases, Rockefeller Branch, The Rockefeller University, New York, NY 10065
[17]Nuffield Department of Clinical Medicine, University of Oxford, Oxford OX3 7BN, England, UK
[18]Centre for Micro-Photonics, Swinburne University of Technology, Hawthorn, Victoria 3122, Australia

In humans, DOCK8 immunodeficiency syndrome is characterized by severe cutaneous viral infections. Thus, CD8 T cell function may be compromised in the absence of DOCK8. In this study, by analyzing mutant mice and humans, we demonstrate a critical, intrinsic role for DOCK8 in peripheral CD8 T cell survival and function. DOCK8 mutation selectively diminished the abundance of circulating naive CD8 T cells in both species, and in DOCK8-deficient humans, most CD8 T cells displayed an exhausted CD45RA$^+$CCR7$^-$ phenotype. Analyses in mice revealed the CD8 T cell abnormalities to be cell autonomous and primarily postthymic. DOCK8 mutant naive CD8 T cells had a shorter lifespan and, upon encounter with antigen on dendritic cells, exhibited poor LFA-1 synaptic polarization and a delay in the first cell division. Although DOCK8 mutant T cells underwent near-normal primary clonal expansion after primary infection with recombinant influenza virus in vivo, they showed greatly reduced memory cell persistence and recall. These findings highlight a key role for DOCK8 in the survival and function of human and mouse CD8 T cells.

CORRESPONDENCE
Christopher C. Goodnow:
chris.goodnow@anu.edu.au

Abbreviations used: APC, allophycocyanin; HIES, hyper-IgE syndrome; HPV, human papillomavirus; MTOC, microtubule-organizing center; TAE, T cell activation and expansion; WAS, Wiskott–Aldrich syndrome.

CD8 T cells have a remarkable capacity for clonal expansion and play an important role in immunity (Masopust et al., 2007). Their essential role in immunity has been demonstrated in mice by genetic or antibody-mediated ablation studies (Doherty, 1996; Harty et al., 2000) and is evidenced in humans by chronic sinopulmonary infections in rare individuals with selective CD8 T cell deficiency caused by homozygous

K.L. Randall, S.S.-Y. Chan, C.S. Ma, and I. Fung contributed equally to this paper.
J. Oliaro, S.G. Tangye, E.M. Bertram, and C.C. Goodnow contributed equally to this paper.

The Rockefeller University Press $30.00
J. Exp. Med. Vol. 208 No. 11 2305-2320
www.jem.org/cgi/doi/10.1084/jem.20110345

Supplemental Material can be found at:
http://jem.rupress.org/content/suppl/2011/10/13/jem.20110345.DC1.html

Published October 17, 2011

mutations in *CD8*, *TAP1*, or *TAP2* (de la Salle et al., 1999; Gadola et al., 2000; de la Calle-Martin et al., 2001) or by the reconstitution of immunity to EBV and CMV with CD8 T cells during transplantation (Walter et al., 1995). A key question in the field is how CD8 T cell differentiation into short-lived cytotoxic effector T cells is balanced against maintaining a persisting pool of CD8 memory T cells with potent recall responses to avoid exhausting the pool of responding T cells and how failure of this process may contribute to chronic viral illness (Intlekofer et al., 2006; Williams et al., 2006a; Sallusto et al., 2010). Answers to this question hold the potential for new interventions to promote long-lived CD8 T cell immunity in vaccination or chronic infection but require experimental studies that bridge human and mouse memory CD8 T cells.

The recent discovery of an immunodeficiency syndrome caused by inactivating mutations in DOCK8 in humans and mice (Engelhardt et al., 2009; Randall et al., 2009; Zhang et al., 2009) provides a unique opportunity to analyze the consequences of this specific molecular perturbation for CD8 T cells in both species. DOCK8 is a member of the DOCK family of intracellular signaling proteins, which are recruited to PIP3 (phosphatidylinositol-trisphosphate)-rich membranes through their DHR1 (Dock homology region 1) domain and serve as guanine exchange factors for Rho/Rac family GTPases through their DHR2 domain (Côté and Vuori, 2007). Other members of this protein family are involved in polarized accumulation of cell adhesion molecules and actin filaments required for cell adhesion, migration, and signaling events (Côté and Vuori, 2007). DOCK8 is most highly expressed in B and T lymphocytes. Individuals with homozygous inactivating DOCK8 mutations present with clinical signs of combined B and T cell immunodeficiency: recurrent sinopulmonary infections typical of humoral immunodeficiency and severe cutaneous viral infections with HSV, human papillomavirus (HPV), and scarring *Molluscum contagiosum* suggestive of T cell dysfunction (Engelhardt et al., 2009; Zhang et al., 2009). These patients also have severe atopy with almost universal atopic dermatitis and sensitization to both foods and aeroallergens. It is likely that DOCK8 mutations account for most of the patients previously classified as having autosomal recessive hyper-IgE syndrome (HIES [AR-HIES]; Engelhardt et al., 2009). Analysis of DOCK8-deficient mice has shown that mutations in this gene cause a partial humoral immunodeficiency, affecting B cells autonomously to prevent long-lasting serum antibody production after immunization. DOCK8-deficient B cells lack normal recruitment of ICAM-1 to the B cell immune synapse, are unable to form marginal zone B cells, and have greatly reduced persistence and affinity maturation of germinal center B cells (Randall et al., 2009).

In contrast, little is known about the effects of DOCK8 deficiency within the T cell lineage in humans or mice. Moderate decreases in circulating T cell numbers have been found in some human DOCK8-deficient patients, although in many others the CD8 T cell count was within the normal range (Engelhardt et al., 2009; Zhang et al., 2009). In vitro stimulation with antibodies to CD3 and CD28 found that CD8 T cells from patients exhibited little or no proliferation compared with healthy controls, whereas CD4 T cell responses were diminished in some patients but relatively normal in others (Engelhardt et al., 2009; Zhang et al., 2009). However, it is unclear to what extent these effects are primary consequences of DOCK8 deficiency in CD8 T cells or secondary to the multiple, recurrent infections afflicting DOCK8-deficient patients or their treatment. For example, responses have yet to be measured in CD8 T cells fractionated with respect to the various naive and memory subsets. The concurrent discovery of *Dock8* mutant mice provides an opportunity to compare the consequences of DOCK8 deficiency in T cells from both species, taking advantage of specific pathogen-free conditions and cell mixing experiments in mice to exclude confounding factors of humoral immunodeficiency and concurrent infections.

In this study, we show that DOCK8 acts cell autonomously in CD8 T cells and that its deficiency causes profound qualitative abnormalities in mice and humans. In humans, the most striking effect is depletion of circulating naive CD8 T cells and accumulation of an exhausted subset of CD8 T cells that are unresponsive to CD3/CD28 stimulation. In mice, the most striking effect is a failure of memory CD8 T cells to persist and mount a recall response after the first wave of CD8 T cell proliferation after influenza infection. The selective failure of memory CD8 T cell persistence parallels the effects of other mutations that affect LFA-1 or TCR concentration at the T cell synapse during initial antigen encounter, and those parallels are borne out here by demonstrating that DOCK8 deficiency diminishes recruitment of LFA-1 to the CD8 T cell synapse with DCs. These results extend and translate to human immunity evidence for an intimate relationship between the quality of the CD8 T cell immune synapse and the generation of long-lived, recallable memory CD8 T cells.

RESULTS

Altered differentiation and impaired proliferation of T cells from DOCK8-deficient humans

To explore the effects of DOCK8 deficiency on T cells, we first analyzed peripheral blood T cells from six DOCK8-deficient patients from five unrelated kindreds. Some of the clinical characteristics of these patients are detailed in Table I. Consistent with a previous study (Engelhardt et al., 2009), the frequency of CD8 T cells within the total lymphocyte population from DOCK8-deficient patients was comparable with that of normal age-matched controls (Fig. 1, A and B). However, when subsets of CD8 T cells were enumerated, there was a dramatic and highly significant loss of naive ($CD45RA^+CCR7^+$) cells ($\sim$10% in patients compared with $\sim$45% in normal controls), together with a smaller but still significant decrease in memory ($CD45RA^-CCR7^{-/+}$) CD8 T cells. Strikingly, the majority of CD8 T cells from DOCK8-deficient patients exhibited a $CD45RA^+CCR7^-$ phenotype

Published October 17, 2011

(Fig. 1, A and B), which is typically associated with cell exhaustion or replicative senescence (Appay et al., 2008). Because of their reexpression of CD45RA, these cells have been termed effector memory CD45RA$^+$ (T_{EMRA}) cells.

For functional analyses, CD8 T cells from the different patients were sorted into populations of either naive (CD45RA$^+$ CCR7$^+$), memory (CD45RA$^-$CCR7$^{-/+}$), or T_{EMRA} (CD45RA$^+$ CCR7$^-$) cells, labeled with CFSE, and stimulated with T cell activation and expansion (TAE) beads, which were coated with mAb to human CD3, CD28, and CD2, in the absence or presence of IL-2. Because of the lymphopenia that is characteristic of DOCK8-deficient patients (Zhang et al., 2009), not all subsets of these cells could be recovered in sufficient numbers from all patients. Consequently, the data presented in Fig. 1 C are a composite derived from experiments performed using subsets of CD8 T cells isolated from different patients. Naive (CD45RA$^+$CCR7$^+$) and memory (CD45RA$^-$ CCR7$^{-/+}$) CD8 T cells from normal controls were induced to undergo multiple rounds of division in response to stimulation with TAE beads, whereas the corresponding subset from DOCK8-deficient patients failed to divide under these stimulatory conditions (Fig. 1 C). Notably, provision of exogenous IL-2 failed to improve proliferation of DOCK8-deficient memory cells (Fig. 1 C). In contrast, there was an absence of a proliferative response by T_{EMRA} cells from either normal donors or patients (Fig. 1 C). This is consistent with previous findings that have investigated the CD8 T_{EMRA} cell subset from normal donors as well as in other clinical settings (Champagne et al., 2001; Brenchley et al., 2003; Geginat et al., 2003; Papagno et al., 2004). The shift of the CD8 T cell compartment toward exhausted T_{EMRA} cells in DOCK8 deficiency reveals a separate effect that complicates interpretation of the role of DOCK8 in human CD8 T cell proliferation.

In contrast to the striking shift in CD8 T cell phenotypic subsets, when the CD4 T cell compartment of DOCK8-deficient patients was examined, although there was a significant reduction in the frequency of CD4 T cells within the lymphocyte population, we found that the distribution of naive (CD45RA$^+$CCR7$^+$) and memory (CD45RA$^-$CCR7$^{-/+}$) subsets in DOCK8-deficient patients resembled that observed for normal controls (Fig. 1, D and E). Despite this, functional analysis of naive and memory CD4 T cells from patients 1 (Fig. 1 F) and 2 (Fig. 1 G) revealed markedly diminished proliferation after stimulation with TAE beads compared with the vigorous division of corresponding CD4 T cell subsets from normal donors. Furthermore, although division of the mutant DOCK8 T cells could be improved by exogenous IL-2, it remained substantially less than that of control cells (Fig. 1, F and G). Thus, DOCK8 deficiency in humans diminishes clonal expansion of both CD4 and CD8 T cells in response to engagement of TCR and costimulatory molecules.

CD8$^+$ T cells in DOCK8-deficient patients have undergone chronic activation in vivo

T_{EMRA} cells have been found to have experienced extensive replication in vivo (Hamann et al., 1999; Dunne et al., 2002; Rufer et al., 2003) yet exhibit poor proliferation in vitro (Champagne et al., 2001; Geginat et al., 2003).

Table I. DOCK8-deficient patients

DOCK8-deficient patients	Age at analysis	*DOCK8* mutation	Effect on protein	Clinical features
	yr			
#1	14	Homozygous 114-kb deletion spanning exons 4–26	Not expressed	Pneumonia, eczema, cutaneous lesions, fungal infections, eosinophilia; IgE 4,800–10,000 IU/ml
#2 (patient ARH012; Engelhardt et al., 2009)	12	Homozygous A→T mutation position 70 in exon 7	Premature stop codon: K271X	Severe *M. contagiosum*, pneumonia, meningitis, eczema; IgE 10,000 IU/ml
#3	4	Homozygous 150-kb deletion	Not expressed	*M. contagiosum* infection (family history)
#4	10	Large homozygous deletion	Not expressed	Recurrent otitis media, eczema, HPV, onychomycosis, *Salmonella*; IgE 1,552 IU/ml; suggestive inflammatory bowel disease and vasculitis
#5	11	Large homozygous deletion	Not expressed	Recurrent upper respiratory tract infection, HPV, *Giardia lamblia*, *Salmonella*; IgE 19,302 IU/ml; inflammatory bowel disease and vasculitis
#6	12	c.3733_3734delAG	Premature stop codon: p.R1245EfsX5	Eczema (with methicillin-resistant *S. aureus* infection), *M. contagiosum*, recurrent otitis media (methicillin-resistant *S. aureus*), multiple food allergies; IgE ∼1,500 IU/ml

Patients #4 and #5 are siblings.

Published October 17, 2011

Furthermore, in the setting of chronic viral infection, these cells may have undergone replicative senescence (Chen et al., 2001; Brenchley et al., 2003; Papagno et al., 2004; Plunkett et al., 2005). A feature of the T_{EMRA} cell population is expression of CD57 on a substantial proportion of these cells (Appay et al., 2008). Interestingly, CD57 expression correlates with both an inability to undergo proliferation in response to either polyclonal or antigen-specific stimulation and heightened susceptibility to apoptosis in vitro (Brenchley et al., 2003). To further analyze CD8 T cell subsets in DOCK8 deficiency and to understand the proliferative defects in these cells, we assessed expression of a range of molecules whose expression is altered during differentiation of naive cells into effector cells (Appay et al., 2008). Compared with naive cells, memory CD8 T cells from normal donors not only acquire expression of CD57, but also dramatically up-regulate CD244 (2B4), CD11a, CD11b, CX3CR1, CD95, and granzyme B and concomitantly down-regulate CD27, CD28, and CD127 (IL-7Rα; Fig. 2 and Fig. S1). Notably, expression of these molecules is substantially increased (CD244, CD11a, CD11b, CD57, CX3CR1, CD95, and granzyme B) or decreased (CD27, CD28, and CD127) on normal T_{EMRA} cells (Fig. 2 and Fig. S1). Remarkably, the levels of expression of these molecules on memory CD8 T cells from DOCK8-deficient patients resembled that of T_{EMRA} cells from normal individuals (Fig. 2 and Fig. S1). Indeed, unlike normal memory and T_{EMRA} cells, there was no significant difference in their levels of expression between DOCK8-deficient memory CD8 T cells and normal T_{EMRA} cells (Fig. 2 and Fig. S1). Furthermore, these molecules were up- or

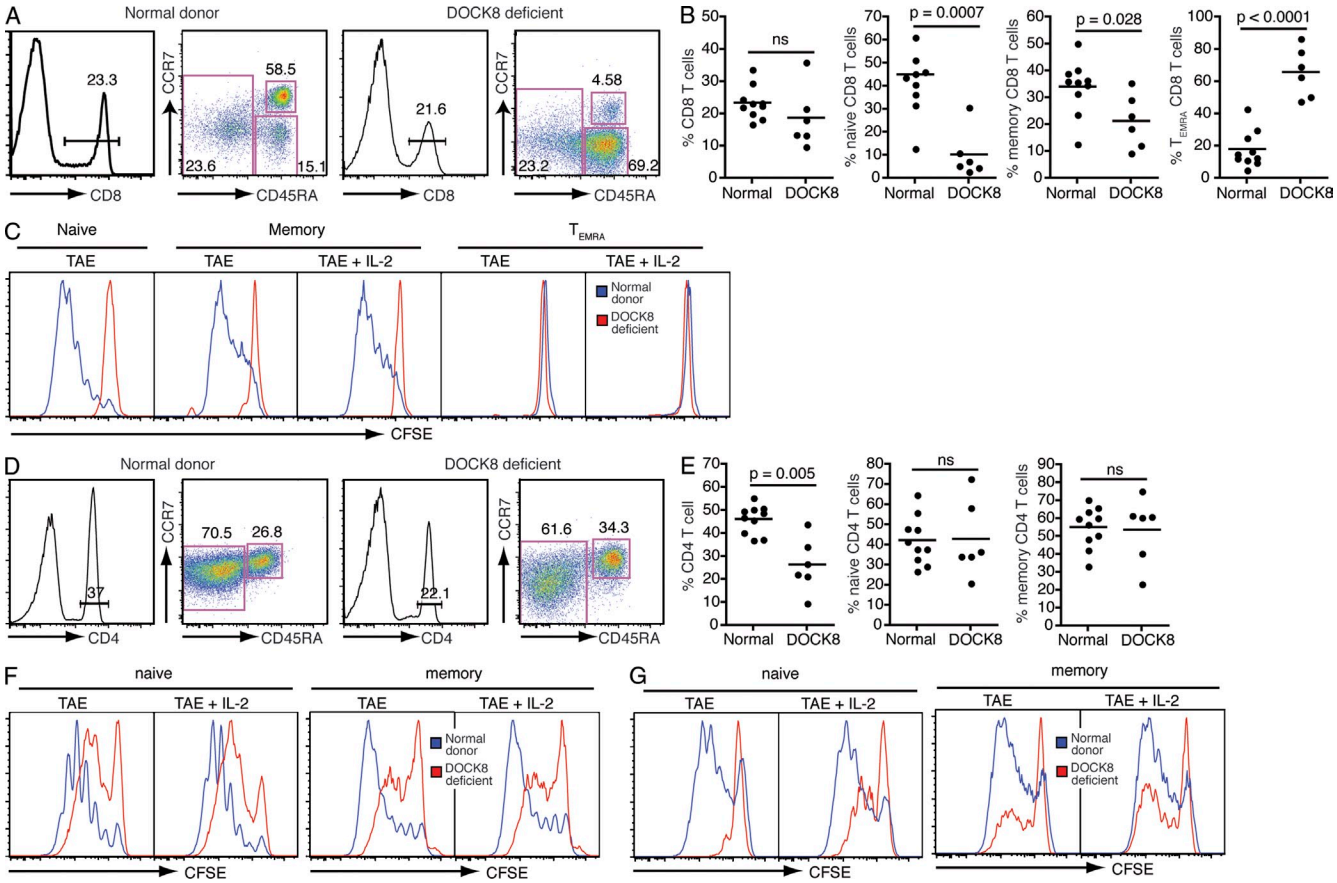

Figure 1. DOCK8 deficiency severely perturbs differentiation and proliferation of naive and memory human T cells. PBMCs from normal donors or DOCK8-deficient patients were analyzed. (A and B) Representative FACS plots and quantitation of total CD8 T cells and naive ($CD45RA^+CCR7^+$), memory ($CD45RA^-CCR7^-$), and T_{EMRA} (effector memory $CD45^+$ [$CD45RA^+CCR7^-$]) cell subsets. The FACS plots in A show one representative normal donor and one DOCK8-deficient patient, whereas the graphs in B show data for all samples analyzed, with the horizontal bars representing the mean frequency of cells with the indicated phenotype. (C) CD8 naive, memory, and T_{EMRA} T cells were isolated from normal donors and patients 1 and 2 (red histograms), labeled with CFSE, and then stimulated with TAE beads in the absence or presence of exogenous IL-2. Cell division was determined after 5 d by measuring dilution of CFSE. (D and E) Representative FACS plots and quantitation of total CD4 T cells and naive ($CD45RA^+CCR7^+$), memory ($CD45RA^-CCR7^-$), and T_{EMRA} ($CD45RA^+CCR7^-$) cell subsets. The FACS plots in D show one normal donor and one DOCK8-deficient patient, whereas the graphs in E show data for all samples analyzed, with the horizontal bars representing the mean frequency of cells with the indicated phenotype. (F and G) $CD4^+$ naive (left) and memory (right) T cells were isolated from normal donors and patients 1 (F) and 2 (G; red histograms), labeled with CFSE, and then stimulated with TAE beads in the absence of presence of exogenous IL-2. Cell division was determined after 5 d by measuring dilution of CFSE. Significant differences were determined by the Student's *t* test.

Published October 17, 2011

down-regulated to a greater extent on DOCK8-deficient T_{EMRA} CD8 T cells compared with corresponding cells from normal donors (Fig. 2 and Fig. S1). Thus, the vast majority (>70%) of DOCK8-deficient T_{EMRA} CD8 T cells exhibited a $CD57^+CX3CR1^+CD27^-CD28^-CD127^-$ phenotype, compared with only 40–50% of normal T_{EMRA} cells which had this phenotype (Fig. 2). Remarkably, even naive CD8 T cells from DOCK8-deficient patients differed phenotypically from normal naive cells inasmuch that they expressed elevated levels of CD11a, CD11b, and CD95 and displayed a mild down-regulation of CD28, CD27, and CD127 (Fig. 2 and Fig. S1). Overall, these data suggest that DOCK8-deficient CD8 T cells have undergone aberrant differentiation in vivo, such that most non-naive cells have acquired an effector/exhausted phenotype, whereas naive cells exhibit features of early activation.

Intrinsic effects of DOCK8 deficiency on circulating naive CD8 T cells

The cell-autonomous role of DOCK8 in T cells was further investigated in specific pathogen-free C57BL/6 mice homozygous for the inactivating *Dock8*$^{pri/pri}$ mutation. These animals inherit a Ser>Pro substitution predicted to disrupt a key α-helix in the Rho/Rac-binding site of the DHR2 domain and have a comparable phenotype with *Dock8*$^{cpm/cpm}$ mice homozygous for a truncating mutation that abolishes over half of the protein (Randall et al., 2009). We first sought to understand the depletion of naive CD8 T cells in human DOCK8 deficiency by focusing on the formation and numbers of circulating naive CD8 T cells in *Dock8*$^{pri/pri}$ mice.

Paralleling the human phenotype, the number of circulating naive CD8 T cells was decreased in *Dock8*$^{pri/pri}$ homozygous mutants (Fig. 3, A and B). CD8 and CD4 T cell subsets were subdivided into naive and activated/memory cells by flow cytometric staining for CD44. Naive $CD44^{lo}$ T cell subsets within both CD8 and CD4 populations were decreased ∼50% in blood, spleen, and LNs of *Dock8*$^{pri/pri}$ mice (Fig. 3, A and B; and Fig. S2). In contrast, the percentages and numbers of activated/memory $CD44^{hi}$ CD8 and CD4 T cells were comparable or slightly increased in DOCK8 mutant animals. Further analysis of the expression of CD45RB, PD-1, CTLA-4, KLRG1, CD127, CD122, CD25, CD27, CD3, or Tbet on the $CD8^+CD44^{hi}$ subset revealed no difference in *Dock8*$^{pri/pri}$ mice compared with normal controls (Fig. S3). Parallel analyses of *Dock8*$^{cpm/cpm}$ mice yielded comparable results (Figs. S3 and S4). These data indicate that DOCK8 deficiency in specific pathogen-free mice also diminishes naive CD8 cells, but in

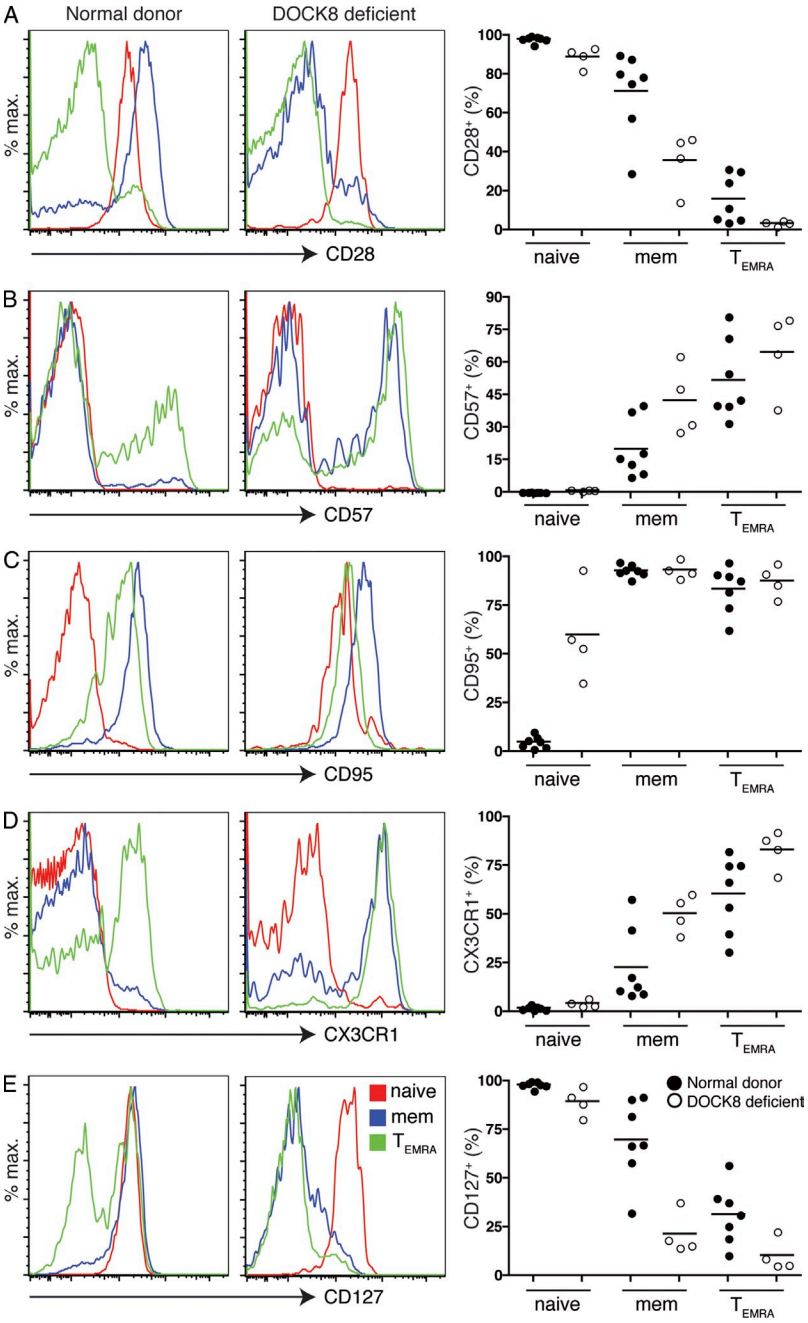

Figure 2. Phenotypic analysis of human DOCK8-deficient CD8$^+$ T cells. (A–E) PBMCs from normal donors (n = 9) or DOCK8-deficient patients (n = 4) were labeled with anti-CD8, anti-CD45RA, and anti-CCR7 mAbs and either isotype control or mAb specific for CD28, CD57, CD95, CD127 (IL-7Ra), and CX3CR1. The expression of these molecules on naive ($CD45RA^+CCR7^+$), memory ($CD45RA^-CCR7^-$), and T_{EMRA} ($CD45RA^+CCR7^-$) cell subsets of CD8 T cells was then determined. The histogram plots are from one representative normal donor or control. Each value in the graphs corresponds to an individual normal donor or patient; the horizontal bars represent the mean.

Published October 17, 2011

this situation it does not result in accumulation of exhausted memory CD8 T cells.

Decreased naive CD8 or CD4 T cells in the periphery of *Dock8*$^{pri/pri}$ mice was not explained by any consistent decrease in the numbers of CD8 or CD4 single-positive T cells in the thymus (Fig. 3 C). In some experiments, there were slightly fewer CD4 and CD8 T cells in the thymus of *Dock8*$^{pri/pri}$ mice (Fig. S5 A), although this was not consistently observed. Further subsetting of mature CD4 and CD8 thymocytes based on expression of CD62L and CD69 revealed slightly decreased frequencies of less mature CD69^{hi}CD4^{+} and CD69^{hi}CD8^{+} cells in *Dock8*$^{pri/pri}$ thymi as a percentage of the total lymphocytes (Fig. 3 D). There was no consistent evidence for accumulation or deficiency of mature CD62L^{+}CD69^{-} single-positive cells (Fig. 3 D and Fig. S5) in the thymus as is observed in animals with defective thymic egress (Matloubian et al., 2004; Carlson et al., 2006; Shiow et al., 2008). Moreover, when the *Dock8*$^{pri/pri}$ mutation was crossed into transgenic mice expressing an MHC I–restricted TCR, OT-I, it caused no discernable decrease in the positive selection of CD8 single-positive T cells bearing this TCR (Fig. 3, E and F). Interestingly, the frequency of naive peripheral CD8 T cells bearing the OT-I TCR was unaffected by the *Dock8*$^{pri/pri}$ mutation. Collectively, these results indicate that DOCK8 deficiency causes only subtle changes in thymic T cell differentiation.

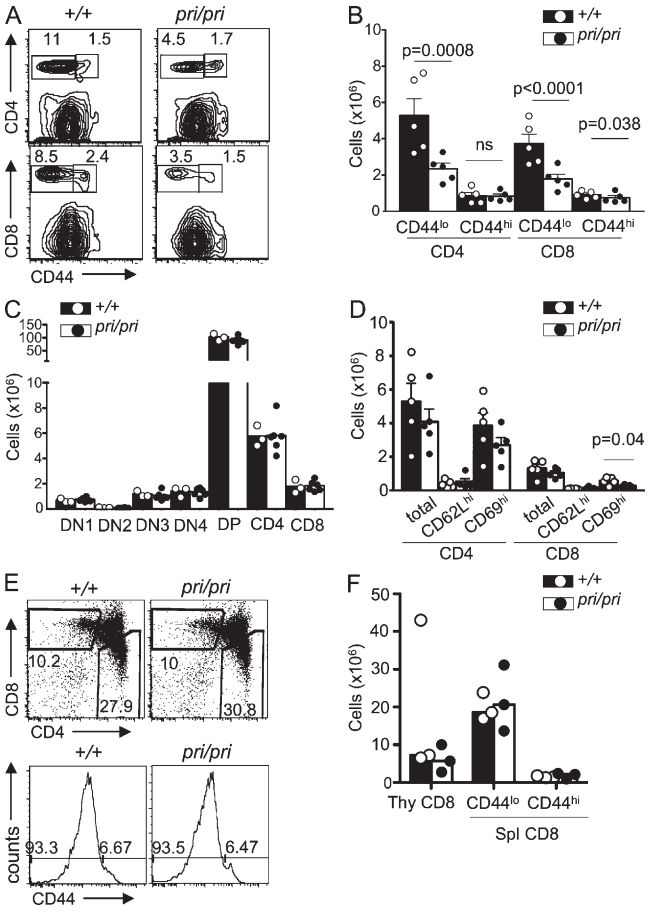

Figure 3. Analysis of T cells in *Dock8*$^{pri/pri}$ mice. (A) Representative flow cytometry plots of T cells in the spleen of *Dock8*$^{pri/pri}$ and C57BL/6 (+/+) mice. (B–D) Quantitation of T cells in spleen (B) and various subsets of thymic T cells (C and D) for age-matched C57BL/6 and *Dock8*$^{pri/pri}$ mice. Bars are means, error bars indicate SEM, and dots indicate individual mice. Statistical analysis was performed by the unpaired Student's *t* test with Welch's correction. Data are representative of three independent experiments. (E) Representative flow cytometry plots of thymic (top) and splenic (bottom) cells from OT-I mice. (F) Quantitation of thymic and splenic CD8 T cells in WT and mutant OT-I mice. Bars are medians, and dots indicate individual mice.

The decrease in naive peripheral CD8 and CD4 T cells could reflect either a cell-autonomous requirement of DOCK8 in these T cell subsets or a secondary effect of abnormalities in other cell types. To distinguish between these alternatives, we constructed mixed bone marrow chimeras by reconstituting irradiated mice with 50:50 mixtures of congenically marked bone marrow from *Dock8*$^{pri/pri}$ CD45.2 and *Dock8*$^{+/+}$ CD45.1 donors. Peripheral B220^{+} cells were reconstituted in almost equal ratios by mutant and WT cells, consistent with previous results demonstrating no effect of the mutation on circulating B cell numbers (Randall et al., 2009) and thereby providing an internal measure for relative engraftment by the two marrow sources in each chimeric animal (reconstitution of individuals shown by bars in Fig. 4 A). In contrast, CD45.2^{+} T cells with defective DOCK8 were dramatically underrepresented in peripheral CD8 and CD4 T cell subsets so that they comprised only 5% of circulating T cells on average. In the same animals, DOCK8 mutant T cells averaged 16% of thymic CD4 and CD8 single-positive T cells, 22% of CD4^{+}CD8^{+} double-positive cells, and 30% of CD4^{-}CD8^{-} double-negative cells. The proportion of peripheral CD45.2^{+} CD8 T cells that were CD44^{hi} in the mixed chimeras was not elevated, comprising ~20% of *Dock8*$^{pri/pri}$ CD8 cells and 18% of *Dock8*$^{+/+}$ CD8 cells (Fig. 4 B). Collectively, these results indicate that DOCK8 deficiency has a subtle cell-autonomous effect on T cells that is compounded at progressive stages of thymic and peripheral T cell formation.

To investigate further the decreased number of naive peripheral CD8 T cells, we adoptively transferred mixtures of congenically marked normal and *Dock8*$^{pri/pri}$ mutant spleen T cells into normal C57BL/6 mice. The survival of these adoptively transferred T cells was then determined by assessing the total number of adoptively transferred cells present as well as the ratio of WT to mutant donor-derived T cells at various time points compared with their ratios at the time of injection. Both WT and mutant T cells slowly declined in frequency up to 39 d after adoptive transfer (Fig. 5, A and B). The contribution of mutant T cells as a percentage of total donor T cells was consistently lower than the input percentage. Similar results were obtained when the transferred WT and *Dock8*$^{pri/pri}$ T cells were obtained from OT-I TCR transgenic mice with a homogeneous TCR specificity: mutant OT-I T cells accounted for 39% of the OT-I cells at the time of transfer but only 20% after 39 d, representing a halving of

Published October 17, 2011

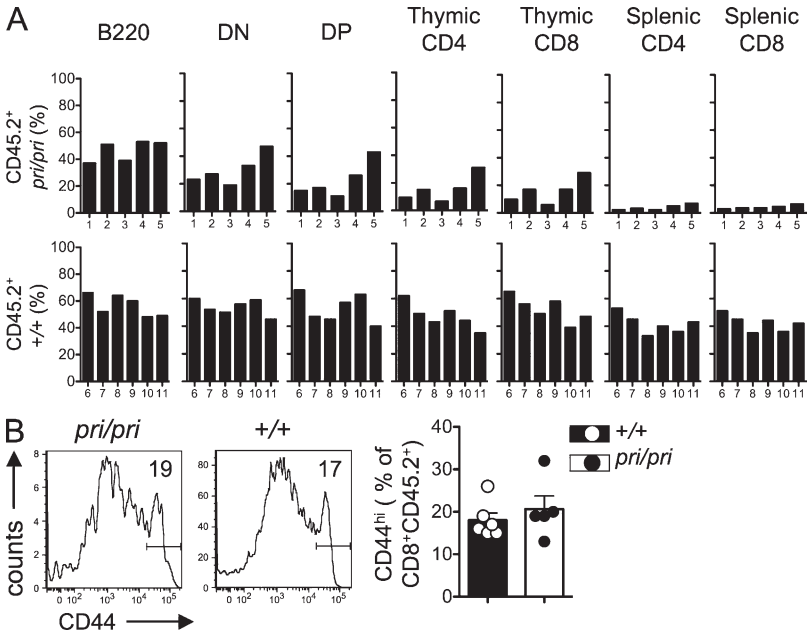

Figure 4. Analysis of bone marrow chimeras. Bone marrow chimeras were reconstituted with 50% *Dock8*$^{pri/pri}$ CD45.2$^+$ and 50% WT CD45.1$^+$ bone marrow. Controls were reconstituted with 50% WT CD45.2 and 50% WT CD45.1 bone marrow. (A) Percentage of CD45.2$^+$ cells reconstituting the cellular subsets shown in these bone marrow chimeras. Each bar is the percent reconstitution of a cell subset in an individual mouse (indicated by the number below the bar). Data are representative of two independent experiments. DN, double negative; DP, double positive. (B) Representative flow cytometry plots and quantitation of CD44 expression on CD45.2$^+$ *pri/pri* and WT (*+/+*) cells from chimeras as in A. Bars are means, error bars indicate SEM, and dots indicate individual mice.

survival over this time period (Fig. 5 B, bottom). We conclude that the persistence of naive peripheral CD8 T cells is intrinsically decreased, albeit modestly, when they lack normal DOCK8. Collectively with the aforementioned normal thymocyte subsets, the reduced peripheral survival provides the simplest explanation for the 50% lower numbers of naive CD8 T cells at steady-state.

We asked whether the decrease in survival of naive CD8 cells lacking normal DOCK8 was caused by a difference in the expression of the α chain of the receptor for IL-7, CD127, or in the T cell response to IL-7. Only a subtle but nevertheless consistent decrease in CD127 expression was observed on naive CD8 and CD4 T cells from *Dock8*$^{pri/pri}$ mice relative to WT littermates (Fig. S6). DOCK8 mutant CD8 and CD4 T cells responded to optimal concentrations of IL-7 in culture with indistinguishable short-term survival relative to WT controls (Fig. S7 A), although they did exhibit a slight decrease in Bcl-2 induction under these conditions (Fig. S7, B and C).

DOCK8 is required for LFA-1 polarization and rapid initiation of cell division

We next examined how DOCK8 deficiency affected CD8 T cell activation. Naive CD8 T cells specific for ovalbumin peptide SIINFEKL presented by H2 K^b were purified from the spleens of OT-I TCR transgenic mice with WT or mutant DOCK8. The T cells were CFSE labeled and co-cultured with SIINFEKL-pulsed bone marrow–derived DCs, and their cell division was followed over a time course by flow cytometry (Fig. 6 A). After 28 h, most of the WT cells had completed their first cell division, whereas few mutant cells had divided at this time point and only completed their first division by 34–40 h. Subsequent divisions nevertheless occurred rapidly so that by 49 h there was little difference between the mutant and WT cells. Addition of exogenous IL-2 did not rectify the delayed first division of DOCK8 mutant T cells (not depicted). In vitro activated *Dock8*$^{pri/pri}$ CD8 OT-I cells had normal cytotoxic activity in chromium release assays (Fig. S8), and normal TNF, IFN-γ, and IL-2 were produced by *Dock8*$^{pri/pri}$ CD8 cells in response to PMA and ionomycin (not depicted). DOCK8-deficient nontransgenic T cells divided almost normally in response to anti-CD3 and CD28 antibodies, although there was again evidence of a slight decrease (not depicted).

To investigate earlier steps in CD8 T cell activation, DOCK8 mutant and WT naive OT-I T cells were purified and co-cultured with SIINFEKL-pulsed DCs as above, and cell conjugates formed after 1 h were fixed and immunofluorescently labeled. Polarization of the microtubule-organizing center (MTOC; identified by tubulin staining) to the T cell–DC interface was used as a marker of immunological synapse formation. Images were obtained by confocal microscopy, and the polarization of proteins important for immune synapse formation was scored, with 3 indicating that the protein of interest was highly polarized to the T cell/DC interface, 0 indicating no polarization, and −3 indicating that the protein of interest was highly polarized away from the T cell–DC interface. LFA-1 was highly polarized to the immune synapse of WT OT-I T cells, whereas *Dock8*$^{pri/pri}$ OT-I T cells mostly showed an even distribution of LFA-1 on the cell surface, indicating a failure of LFA-1 polarization to the synapse (Fig. 6, B and C). DOCK8 mutant CD8 T cells also failed to polarize actin to the synapse, whereas polarization of PKC-θ occurred relatively normally (Fig. 6, D–G). Together these results indicate that DOCK8 is required to form a normal T cell immune synapse with antigen-presenting DCs.

DOCK8 is required for persistence of memory CD8 T cells

To extend the aforementioned results and examine how DOCK8 mutation affects CD8 T cell clonal expansion and memory cell persistence in vivo after a viral challenge, OT-I T cells with either normal or defective DOCK8, distinguishable by CD45.1 and CD45.2 allelic markers, were mixed, and 1,000 of each were cotransferred into normal C57BL/6 mice.

Published October 17, 2011

At the same time, the recipient mice were injected i.p. with a modified influenza virus that produces the SIINFEKL peptide incorporated within the neuraminidase stalk. Thus, the transferred OT-I T cells will receive help from, and compete with, normal T cells recognizing other components of the virus in the recipient mice so that DOCK8 deficiency will be specifically limited to half of the transferred OT-I T cells. In addition to testing the cell-autonomous function of DOCK8 in CD8 T cells, any mouse to mouse variation in viral exposure or kinetics of the response could be internally controlled by directly comparing the ratio of the cotransferred OT-I T cells within a single animal. Primary and secondary viral challenges of the recipients were performed with two separate influenza strains, H3N2 (HKx31) and H1N1 (PR8), both expressing the SIINFEKL peptide, to recall memory CD8 T cell responses against the virus and the ovalbumin peptide without interference by neutralizing antibodies against viral envelope proteins (Jenkins et al., 2006).

Flow cytometric analysis of lymphocytes from spleen, peritoneal cavity, and bone marrow was used to enumerate the transferred mutant and WT OT-I CD8 T cells (Fig. 7 A). Both DOCK8 mutant and WT OT-I CD8 T cells increased >1,000-fold in response to viral antigen challenge.

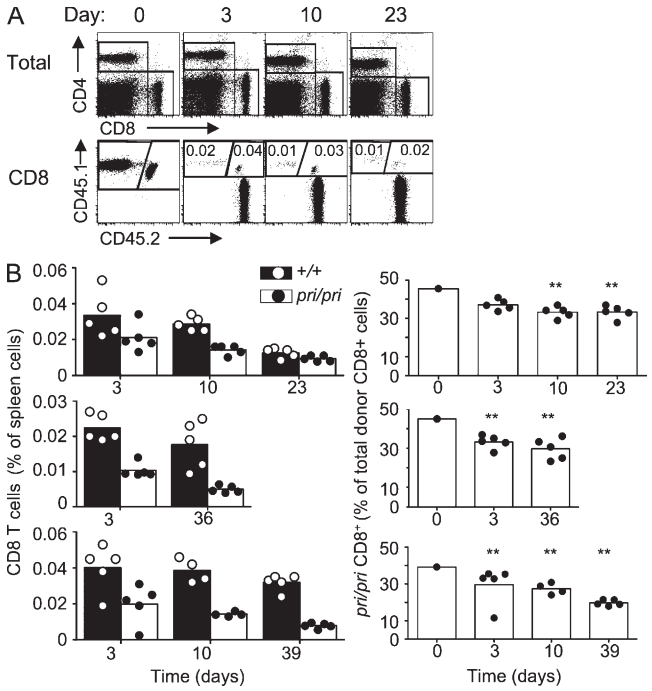

Figure 5. Survival of naive *Dock8*$^{pri/pri}$ T cells. WT (CD45.1/CD45.2) and *Dock8*$^{pri/pri}$ (CD45.1) spleen cells were adoptively cotransferred into normal C57BL/6 mice (CD45.2). (A) Representative flow cytometry plots showing the percentage of adoptively transferred CD8 T cells at various time points after transfer. Numbers indicate the percentage of cells in the gate as a percentage of total spleen cells. (B) Quantitation of adoptively transferred CD8 T cells in two separate experiments using polyclonal T cells (top two panels) and one experiment using OT-I transgenic T cells (bottom). Data are representative of two separate experiments for each cell type. **, $P < 0.01$ for χ^2 test compared with input percentages.

The DOCK8 mutant T cells clonally expanded almost as well as the normal controls in the same animals 7 d after the first viral challenge, although there was a subtle but consistent decrease in each animal reproduced across many experiments (Fig. 7 B). Thus, the mutant OT-I CD8 T cells represented ~35% of all donor-derived OT-I CD8 T cells in the spleen, peritoneal cavity, and bone marrow at day 7 after infection, compared with 45% of the donor cells at the time of adoptive transfer (Fig. 7 B, bottom). This result extends the aforementioned in vitro proliferation experiments and establishes that DOCK8 deficiency causes only a subtle decrease in the net proliferation of CD8 T cells in response to viral antigen in vivo.

By 28 d after the first viral challenge, when viral antigen had been cleared, the OT-I CD8 T cells with WT DOCK8 had decreased in number in the spleen to ~30% relative to their peak numbers at day 7 (Fig. 7 B). In contrast, DOCK8 mutant OT-I T cells in the same animals decreased to 5% of their peak number so that they now represented only 10% of the overall donor-derived OT-I CD8 T cells (Fig. 7 B, bottom). When memory T cells against the virus and the SIINFEKL peptide were restimulated by a second viral infection on day 35, both WT and DOCK8 mutant OT-I CD8 T cells increased in numbers relative to day 28. Despite this, the recall response by the mutant memory T cells was less so that they failed to reach the numbers of the first exposure and accounted for only 5% of the OT-I CD8 T cells at the height of the recall response. The difference between the normal and DOCK8-defective T cells could not be explained by preferential movement of mutant OT-I cells into the bone marrow or peritoneum, as comparable differences occurred in the spleen, bone marrow, and peritoneum (Fig. 7 B). The possibility that *Dock8*$^{pri/pri}$ OT-I T cells were selectively rejected because of minor histoincompatibility, either as a result of the DOCK8 mutation, other linked mutations, or the CD45.1 marker, was ruled out by performing parallel adoptive transfers with CD45.1 OT-I control cells that were either *Dock8*$^{pri/+}$ heterozygous or WT (Fig. 7 C). The persistence and recall of both types of control OT-I T cells was equal to their cotransferred CD45.1/2 WT cells, whereas again there was greatly reduced persistence and recall of CD45.1 OT-I T cells that were homozygous for the *Dock8* mutation.

Another possible explanation for the failure of DOCK8-defective CD8 T cells to persist after antigen-induced clonal expansion would be that they selectively formed short-lived effector cells but not cells with the phenotypic markers of memory CD8 T cells. To investigate this possibility, we examined the expression of several markers of CD8 T cell activation and memory cell formation. Surface expression of CD44, CD62L, CD127, and KLRG1 was indistinguishable between mutant and WT OT-I cells at all time points (Fig. 8 A), indicating that there was no measurable difference in the proportion of effector cells or absence of any phenotypically defined memory cell subsets to explain the failure of DOCK8 mutant cells to persist. Slightly lower expression of Bcl2 and Bim was observed in mutant OT-I cells on day 7 of the

Published October 17, 2011

primary influenza response, but this did not reach statistical significance in one of two experiments (not depicted).

To define the role of DOCK8 in the persistence and recall of memory CD8 T cells over longer time periods, the cotransfer of OT-I T cells with normal or defective DOCK8 was repeated with a 6-mo delay between the primary H3N2 and secondary H1N1 SIINFEKL influenza exposure. To directly relate the data from primary, memory, and recall phases, a single cohort of recipient mice was followed longitudinally by measuring the transferred OT-I T cell frequency in their blood (Fig. 8 B). As before, there was only a subtle decrease in expansion of mutant OT-I T cells 7 d after the first viral exposure and a much more rapid decline of mutant T cells after this first antigen was cleared. However, by 195 d, the numbers of DOCK8-deficient OT-I T CD8 cells fell below the limit of reliable enumeration in all of the animals analyzed. In contrast, at the same time point, OT-I T cells with normal DOCK8 were still readily detected in the blood of three of the five recipient mice. In these animals, a large CD8 T cell recall response was made 7 d after reexposure to SIINFEKL influenza (day 202), with the numbers of OT-I T cells increasing 100-fold relative to day 195 immediately before reexposure and 10-fold relative to the peak of the primary response on day 7. Although DOCK8 mutant T cells also increased in these animals, they comprised <1% of the secondary response. Thus, DOCK8 mutation in T cells causes only a subtle decrease in the initial virus-induced clonal expansion of CD8 T cells in vivo but severely compromises the long-term persistence and recall of their memory CD8 progeny.

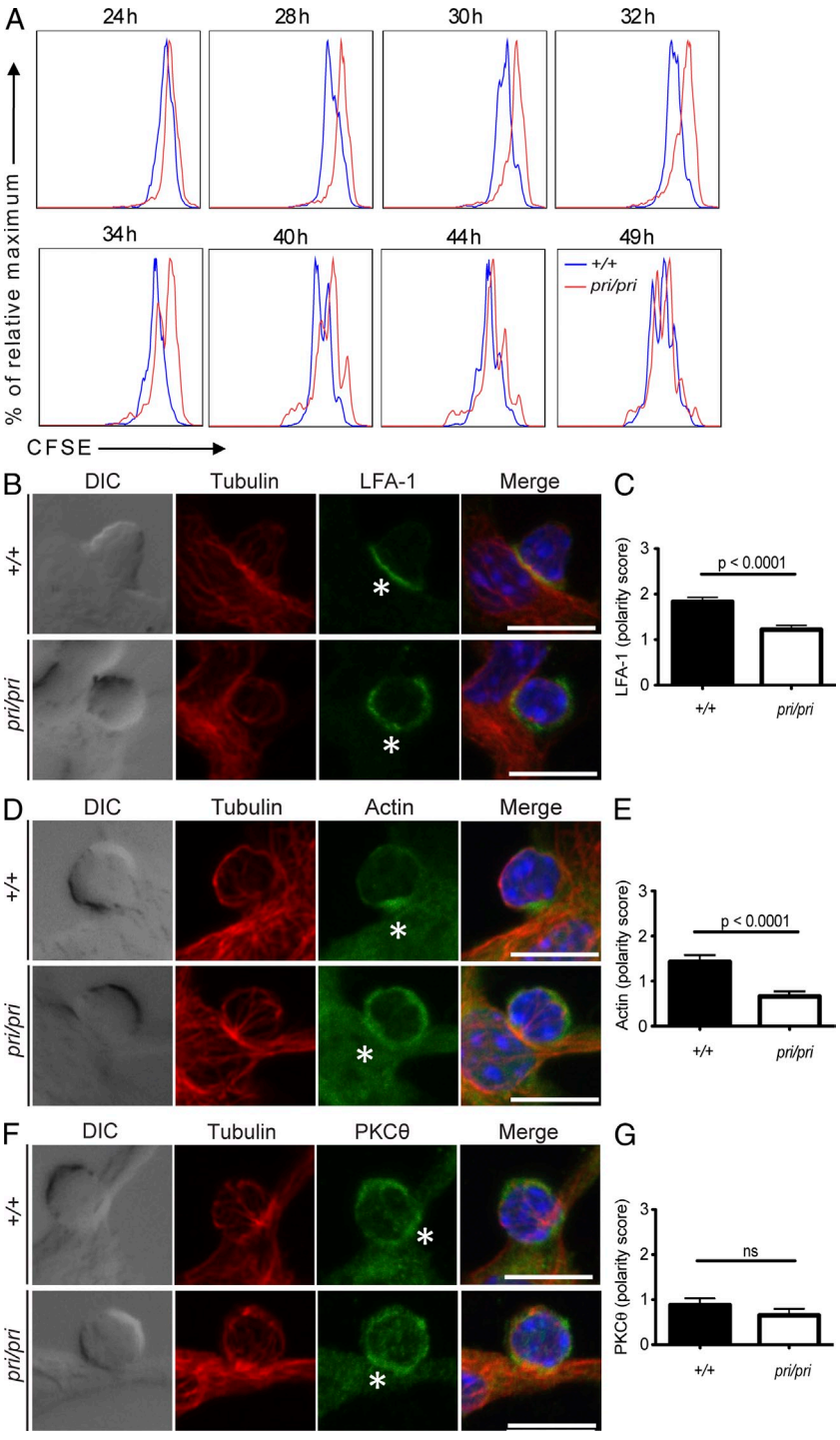

DISCUSSION

Our findings define a qualitative deficit in CD8 T cells caused directly by DOCK8 deficiency. Interpreting the consequences of DOCK8 mutation in CD8 T cells in

Figure 6. *Dock8*$^{pri/pri}$ OT-I T cells show delayed proliferation and a defect in immune synapse formation in response to antigen presentation. (A) Naive WT and *pri/pri* splenic CD8 T cells were labeled with CFSE and cultured with SIINFEKL-pulsed DCs. Cells were harvested at the indicated time points and analyzed for fluorescent intensity of CFSE by flow cytometry. Data are representative of five independent experiments. (B–G) Naive WT and *pri/pri* splenic CD8 T cells were co-cultured with preadhered SIINFEKL-pulsed DCs for 1 h and fixed for immunofluorescence staining. (B, D, and F) Tubulin (red) staining was used to mark recruitment of the MTOC to the immune synapse along with costaining for the protein of interest (green). Images are representative of three independent experiments. Bars, 10 µm. (C, E, and G) Scoring of LFA-1 (+/+, $n = 168$; *pri/pri*, $n = 176$), actin (+/+, $n = 70$; *pri/pri*, $n = 77$), and PKC-θ (+/+, $n = 50$; *pri/pri*, $n = 46$) recruitment to the interface between the T cell and DC (marked by asterisks). Bars are mean, and error bars indicate SD. Scoring was performed blind as per Materials and methods. Statistical analysis was performed by the Student's *t* test.

Published October 17, 2011

DOCK8-deficient humans is complicated by their humoral immunodeficiency, varying degrees of lymphopenia, concurrent infections, and antibiotic and antiviral medication.

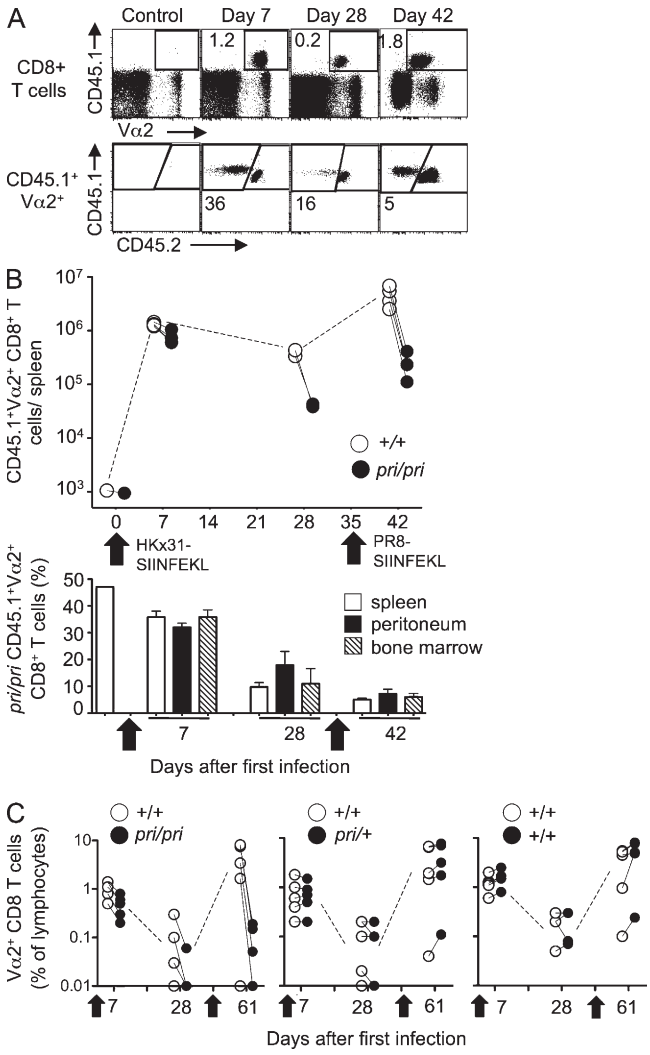

Figure 7. Pairwise analysis of persistence of *Dock8*$^{pri/pri}$ CD8 T cells after viral challenge. OT-I (Vα2$^+$) T cells with either WT or mutant DOCK8 were mixed in a defined ratio and cotransferred into C57BL/6 mice, which were then injected i.p. with modified influenza virus (first HKx31-SIINFEKL and then PR8-SIINFEKL), as indicated by the black arrows. (A) Representative flow cytometry plots showing identification of transferred cells at various time points. Control indicates no adoptive transfer. (B) Time course of adoptive transfer and infection. Graphs show numbers of transferred WT (open) and *Dock8*$^{pri/pri}$ (closed) cells at various time points within the same recipient mouse (top) and percentage contribution of mutant cells to total donor cells within spleen (open), peritoneum (closed), and bone marrow (striped; bottom). For the bottom panel, bars are means, and error bars indicate SEM. Data are representative of two independent experiments. (C) Adoptive transfers as in A and B with three experimental groups. Recipients were injected with *Dock8*$^{pri/pri}$ and WT (+/+) cells, *Dock8*$^{pri/+}$ and WT (+/+) cells, or WT combined with WT cells. Graphs show numbers of transferred WT (open) and either *Dock8*$^{pri/pri}$ (left), *Dock8*$^{pri/+}$ (middle), or WT (right panel; all closed) cells at various time points in the same recipient mouse.

Our analysis has identified an important confounding factor, namely that many of the circulating CD8 T cells correspond to a CD45RA$^+$CCR7$^-$ exhausted T_{EMRA} cell subset that is poorly responsive even in normal individuals. Furthermore, many of the CD45RA$^-$ memory CD8$^+$ T cells in these patients exhibited phenotypic and functional features of such exhausted cells. This phenotype is likely to reflect the repeated viral exposure faced by these patients, as has been observed in patients with other chronic infections such as late stage HIV (Chen et al., 2001; Brenchley et al., 2003) and patients with EBV-positive X-linked lymphoproliferative disease (Plunkett et al., 2005). We also found that DOCK8 deficiency in human T cells abrogated the robust

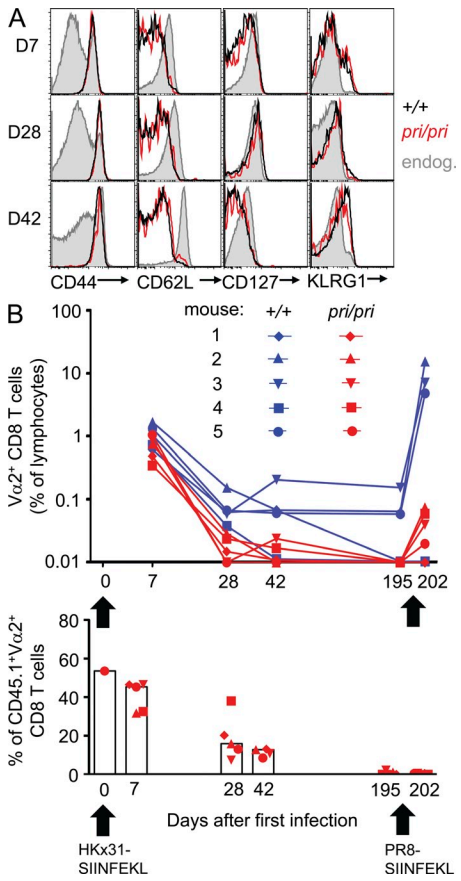

Figure 8. Further investigation of the consequences of DOCK8 deficiency for persistence and recall of primed OT-I CD8 T cells. OT-I T cells with either WT or mutant DOCK8 were mixed in a defined ratio and cotransferred into C57BL/6 mice, which were then injected i.p. with modified influenza virus, as indicated by the black arrows. (A) Overlay histograms of the expression of surface markers on WT (black) and *Dock8*$^{pri/pri}$ (red) donor and recipient (gray) CD8 T cells at the indicated time points after adoptive transfer. (B) Longitudinal time course of adoptive transfer and infection. Graphs show percentages of transferred WT (blue) and *Dock8*$^{pri/pri}$ (red) OT-I CD8 T cells in blood at various time points within the same recipient mouse (denoted by different symbols; top) and percent contribution of mutant cells to total donor cells at various time points after adoptive transfer (bottom). Bars are medians, and dots indicate individual mice. Results of one independent experiment are shown.

Published October 17, 2011

proliferative response observed for normal CD4 and CD8 T cells after stimulation through the TCR and co-stimulatory molecules. This most likely reflects the advanced level of activation of these cells in vivo as a result of chronic pathogen exposure, which can cause extensive proliferation resulting in replicative senescence (Brenchley et al., 2003; Papagno et al., 2004). Indeed, a study of human $CD8^+$ T cell subsets found that expression of CD57 correlates with impaired proliferation and increased susceptibility to apoptosis in vitro (Brenchley et al., 2003). Similarly, $CD8^+$ T cells that are $CD57^+$ (Brenchley et al., 2003), $CD57^+CCR7^-CD27^-$ (Papagno et al., 2004), or $CD45RA^+CCR7^-CD27^-CD28^-$ (Rufer et al., 2003; Romero et al., 2007) have undergone the greatest levels of expansion in vivo, as determined by quantitation of TCR excision circles or telomere lengths, yet fail to proliferate in vitro in response to TCR-mediated stimulation. Furthermore, exogenous cytokines failed to restore the proliferative defect of $CD57^+CD8^+$ human T cells (Brenchley et al., 2003). Thus, the defects in proliferation of all DOCK8-deficient $CD8^+$ T cell subsets is consistent with an enrichment in the frequency of $CD57^+CD27^-CD28^-$ cells within both the memory and T_{EMRA} cell subsets, as well as unusually high expression of CD95 by naive cells.

When DOCK8 deficiency was confined to a subset of the CD8 T cell repertoire in specific pathogen-free mice, we were able to establish an essential, intrinsic role for DOCK8 in CD8 T cells that has its most dramatic effects on the persistence and recall of antigen-stimulated memory CD8 T cells. These effects, together with the effects of DOCK8 deficiency on LFA-1 polarization at the CD8 T cell synapse and on initial entry into cell division, extend and translate to human immunity a growing body of evidence that normal CD8 T cell memory depends on the quality of stimuli received through the T cell synapse before the first cell division.

DOCK8 was found not to be essential for thymic production of T cells, with normal numbers of single-positive CD8 and CD4 cells, no evidence for a defect in CD8 cell–positive selection in OT-I transgenic mice, and modest competitive decreases in all thymic subsets in 50:50 chimeras. Although we have not directly measured thymic egress, there was no consistent evidence for either accumulation or deficiency of mature $CD69^-CD62L^+$ single-positive T cells in the thymus as occurs in animals with thymic egress defects (Matloubian et al., 2004; Carlson et al., 2006; Shiow et al., 2008). DOCK8 played a greater role in peripheral CD8 T cells, with mutation of *DOCK8* decreasing the number of naive T cells by 50%. The numbers of activated/memory $CD44^{hi}$ CD8 T cells were nevertheless slightly increased, presumably because these were sustained by antigen-driven or homeostatic proliferation (Surh and Sprent, 2008). In competitive bone marrow chimeras, 95% of the peripheral CD8 T cells were derived from the normal rather than the mutant bone marrow, and there was no relative shift toward $CD44^{hi}$ T cells among the DOCK8 mutant T cells. Cell transfers show that DOCK8-deficient naive CD8 T cells persist less well in peripheral lymphoid tissues and that influenza-activated OT-I T cells exhibited a persistence defect (70% decline in contribution to transferred OT-I cells over 21 d between days 7 and 28; Figs. 7 B and 8 B) that appears more severe than the survival defect exhibited by unstimulated OT-I cells bearing the mutation (50% decline in contribution to transferred OT-I cells over 39 d; Fig. 5 B). A subtle decrease in CD127 expression and IL-7–induced Bcl-2 was observed in DOCK8 mutant naive T cells and could theoretically explain the subtle decrease in their survival in vivo, but future studies will be needed to address how DOCK8 deficiency affects this pathway. The more dramatic decrease in memory CD8 T cell survival was not accompanied by any measurable decrease in CD127 expression, and only a marginal decrease in Bcl-2. Elucidating the molecular pathway by which DOCK8 promotes survival of naive and memory CD8 T cells and how this may relate to the synapse defect will be challenging given the many gaps in current understanding of the signals that induce long-lived memory T cells. Regardless of its molecular basis, this intrinsic defect in naive and memory T cell persistence coupled with uncontrolled viral infections provides an explanation for the markedly decreased frequency of circulating naive CD8 T cells and the dramatic shift to $CD8^+$ $CD45RA^+CCR7^-$ T_{EMRA} cells in DOCK8-deficient patients.

Although the experiments here establish that DOCK8 deficiency causes a striking qualitative deficit in CD8 T cells, it is unlikely that the CD8 T cell defect alone accounts for the peculiar spectrum of viral infections and tissue-tropism seen in DOCK8 deficiency. Bone marrow transplantation resolved the cutaneous viral infections in two DOCK8-deficient patients, indicating that hematopoietic rather than epidermal defects are responsible (Bittner et al., 2010; Gatz et al., 2011). Deficiency of the skin-homing subset of CD8 T cells is unlikely to explain the cutaneous infections because we find normal frequencies of skin-homing $CD103^+$ CD8 T cells in the skin and gut of DOCK8 mutant mice (unpublished data), as well as in the circulation of DOCK8-deficient patients (unpublished data). It is significant that cutaneous infections with HSV, HPV, and *M. contagiosum* are much less prevalent in severe combined immunodeficiency or selective CD8 T cell deficiency, indicating that the CD8 T cell defects defined here are unlikely to be sufficient to explain the prevalence of these viral infections in DOCK8 deficiency (Laffort et al., 2004; Cerundolo and de la Salle, 2006; Notarangelo et al., 2009). Uncontrolled cutaneous infections with many of the same viruses are associated with evidence for greatly exaggerated Th2 cell activity in otherwise normal individuals with atopic dermatitis, asthma, and food allergy (Wollenberg et al., 2003; Beck et al., 2009). In this setting, Th2 cytokines are believed to suppress Th1 cells and IFN-γ production in the skin, thereby reducing control of these cutaneous viral infections by CD8 T cells and NK cells. Thus, it is attractive to speculate that in AR-HIES caused by DOCK8 deficiency, the effects of excessive Th2 cells interact with the qualitative defect in CD8 T cells to produce the severe HSV, *M. contagiosum*, and other skin viral infections. In contrast, autosomal dominant HIES (AD-HIES) caused by *STAT3* mutations

Published October 17, 2011

results in mucocutaneous infections with *Candida albicans* and cutaneous infection with *Staphylococcus aureus* rather than uncontrolled viral infections. AD-HIES is associated with defective Th17 cells (de Beaucoudrey et al., 2008; Ma et al., 2008; Milner et al., 2008; Renner et al., 2008) and perhaps other cell or cytokine defects, which result in this specific infectious susceptibility.

Patients with another primary immunodeficiency that causes qualitative T cell abnormalities, Wiskott–Aldrich syndrome (WAS), share some clinical characteristics with DOCK8 immunodeficiency patients in that they have eczema, a similar range of infections with *M. contagiosum* and papilloma and herpes viruses (Atherton et al., 2004), and elevated levels of IgE (Bosticardo et al., 2009). The WAS protein is important for T cell synapse formation (Dupré et al., 2002; Badour et al., 2003; Cannon and Burkhardt, 2004), and its expression in DCs is important for interactions between naive CD8 T cells and DCs (Pulecio et al., 2008). It had been previously assumed that the cutaneous infections in WAS were secondary to the eczema (Bosticardo et al., 2009), but the similarities between the clinical manifestations and cellular consequences of WAS protein and DOCK8 deficiency support a link between susceptibility to these viral infections and the presence of a qualitative CD8 T cell synapse defect. A similar spectrum of viral infections (papillomavirus and *M. contagiosum*) is also seen in epidermodysplasia verruciformis (Casanova and Abel, 2007). This primary immunodeficiency occurs because of mutations in *EVER1* and *EVER2* (Ramoz et al., 2002), disrupting zinc transport in keratinocytes, with increased zinc concentrations in the nucleus aiding papillomavirus replication (Lazarczyk et al., 2008). However, the molecular mechanism underlying susceptibility to a similar spectrum of infections in DOCK8 deficiency and EVER-1/2 deficiency is distinct because DOCK8 patients do not have intrinsic abnormalities of their keratinocytes as bone marrow transplantation has been associated with resolution of chronic viral infections (Bittner et al., 2010; Gatz et al., 2011).

Although the initial clonal expansion of DOCK8-deficient OT-I CD8 T cells in response to influenza-produced antigen was almost equal to their paired OT-I WT T cells, the persistence of mutant CD8 T cells after antigen was cleared was greatly diminished, and they exhibited poor secondary expansion upon reexposure to a CD8 T cell cross-reacting influenza strain. The preferential effect of DOCK8 mutation on the persistence and recall of CD8 memory T cells has parallels with several other studies (Williams et al., 2006b; Scholer et al., 2008; Teixeiro et al., 2009). Like DOCK8-deficient CD8 T cells, IL-2Ra–deficient CD8 T cells also show normal primary expansion upon viral challenge in vivo but are greatly decreased in their secondary clonal expansion upon reexposure to antigen (Williams et al., 2006b). However, *Il2ra* deficiency differs because it does not accelerate the loss of antigen-specific CD8 T cells during the contraction phase after the primary response. OT-I T cells bearing a mutation in the TCR β-chain transmembrane domain resemble DOCK8-deficient OT-I cells more closely (Teixeiro et al., 2009). The TCR-β mutation selectively interfered with clustering of the TCR and PKC-θ at the T cell synapse with antigen-presenting cells and the activation of NF-κB. When the TCR-β mutant OT-I T cells were adoptively transferred into mice infected with *Listeria monocytogenes* expressing ovalbumin antigen, the primary clonal expansion was comparable with normal OT-I T cells, but the mutant T cells subsequently declined more rapidly and made little recall expansion upon a second challenge (Teixeiro et al., 2009). The behavior of $Dock8^{pri/pri}$ OT-I T cells most closely resembles normal CD8 OT-I T cells stimulated by ICAM-1–deficient DCs (Scholer et al., 2008). Using normal and $Icam1^{-/-}$ mice, Scholer et al. (2008) adoptively transferred normal OT-I T cells and then immunized them with anti-DEC205 mAb coupled to ovalbumin with or without antagonistic anti-CD40 mAb. Upon immunization, the primary clonal expansion of OT-I T cells was comparable in the two groups, but during the contraction phase, most of the OT-I T cells were lost in the $Icam1^{-/-}$ mice, and little recall clonal expansion occurred upon rechallenge. Two-photon microscopy revealed a failure to form long-lived contacts between T cells and $Icam1^{-/-}$ DCs, consistent with other evidence that prolonged contact with antigen is important for the formation of CD8 memory T cells (Bachmann et al., 2006). Based on the findings here and studies of other DOCK proteins (Côté and Vuori, 2007), DOCK8 deficiency in OT-I T cells may interfere with the inside-out signals needed to activate LFA-1 binding to ICAM-1 on DCs and to promote actin filaments that polarize LFA-1/ICAM-1 at the synapse.

The similarities between the effects of DOCK8 deficiency, ICAM-1 deficiency, and TCR-β mutation provide three independent lines of experimental evidence connecting the quality of the TCR synapse and the intracellular signals it generates with the persistence of memory CD8 T cells. Given the delay to first cell division caused by DOCK8 deficiency in mice and the impaired proliferation of T cells from DOCK8-deficient patients, it is conceivable that qualitative differences in TCR signals are imprinted or stored in the T cell during the period leading up to the first cell division and then passed on silently through the rapid successive divisions to become apparent only when the cells exit cycle and need to persist as nondividing memory cells (Mercado et al., 2000; Kaech and Ahmed, 2001; van Stipdonk et al., 2001). Further analysis of DOCK8 deficiency in man and mouse will help to establish general principles for persistence of CD8 T cell–mediated immunity, to guide new strategies for enhancing this arm of immunity in chronic viral diseases and cancer and for suppressing CD8 T cell memory in transplantation.

MATERIALS AND METHODS

Mice. Mice were housed in specific pathogen-free conditions, and all experiments were approved by the Australian National University Animal Ethics and Experimentation Committee. $Dock8^{pri/pri}$ mice were generated as previously described (Randall et al., 2009). C57BL/6 and C57BL/6.SJL-CD45.1 mice were obtained from Australian National University Bioscience Services. OT-I mice on the C57BL/6 background (Hogquist et al., 1994)

Published October 17, 2011

were provided by F. Carbone (The University of Melbourne, Parkville, Victoria, Australia) and were crossed with *Dock8*$^{pri/pri}$ or *Dock8*$^{+/+}$ B6.CD45.1 mice to obtain OT-I transgenic offspring that were either *Dock8*$^{pri/pri}$ CD45.1 homozygous or *Dock8*$^{+/+}$ CD45.1/CD45.2 heterozygous.

Procedures. Bone marrow chimeras were generated as previously described (Randall et al., 2009). For adoptive transfers, C57BL/6 recipient mice were injected intravenously with 10^3 FACS-sorted OT-I CD8 T cells (50:50 mixture of *Dock8*$^{pri/pri}$ CD45.1 homozygous and *Dock8*$^{+/+}$ CD45.1/2 heterozygous CD8 T cells). For influenza challenge experiments, the mice were also injected i.p. with H3N2 (A/HKx31) followed later by H1N1 (A/PR8) strains of recombinant influenza A viruses expressing SIINFEKL OVA257-264 (Jenkins et al., 2006) obtained from S. Turner (The University of Melbourne).

Flow cytometry of murine cells. Single cell suspensions of spleen, LN, and bone marrow were obtained as described previously (Randall et al., 2009). Data were acquired on a FACSCalibur (BD), FACS Sort (BD), or LSRII (BD) flow cytometer and analyzed using FlowJo software (Tree Star). The following antibodies were used for surface staining of lymphocytes for flow cytometry (from BD unless otherwise stated; clones indicated): FITC-conjugated anti-CD4 (GK1.5), peridinin chlorophyll protein (PerCP)–cyanine (Cy) 5.5–conjugated anti-CD4 (RM4.5), PE-indotricarbocyanine (PE-Cy7)–conjugated anti-CD4 (RM 4.5), allophycocyanin (APC)-conjugated anti-CD4 (RM 4.5), APC-Cy7–conjugated anti-CD4 (GK1.5; BioLegend), PE-conjugated anti-CD4 (GK1.5), PE-conjugated anti-CD8a (53–6.7), PerCPCy5.5-conjuated anti-CD8a (53-6.7), Alexa Fluor 405–conjugated anti-CD8a (5H10; Invitrogen), APC–Alexa Fluor 750–conjugated anti-CD8a (53-6.7, 5H10), PE-Cy7–conjugated anti-CD8a (53-6.7; BioLegend), APC-conjugated anti-CD25 (PC61), APC-Cy7–conjugated anti-CD25 (PC61; BioLegend), PE-conjugated anti-CD27 (LG.3A10), APC-conjugated anti-CD44 (1M7), Alexa Fluor 405–conjugated anti-CD44 (1M7; Invitrogen), Pacific blue–conjugated anti-CD44 (IM7; BioLegend), PE-conjugated anti-CD45.1 (A20), Alexa Fluor 700–conjugated anti-CD45.1 (A20; BioLegend), Pacific blue–conjugated anti-CD45.2 (104; BioLegend), FITC-conjugated anti-CD45.2 (104), APC-conjugated anti-CD45.2 (104; eBioscience), FITC-conjugated anti-CD62L (MEL-14), APC-Cy7–conjugated anti-CD62L (MEL-4; BioLegend), PerCPCy5.5-conjugated anti-CD69 (H1.2F3), FITC-conjugated anti-CD122 (5H4), PE-indodicarbocyanine (PE-Cy5)–conjugated anti-CD127 (A7R34; eBioscience), PE-conjugated anti-CD152 (UC10-4F10-11), FITC-conjugated anti-B220 (RA3-6B2), APC–Alexa Fluor 750–conjugated anti-B220 (RA3-6B2; Invitrogen), APC-conjugated anti-KLRG1 (2F1; eBioscience), PE-conjugated anti-TCR Vα2 (B20.1), FITC-conjugated anti-CD45RB (16A), PE-conjugated anti-PD-1 (J43), and Alexa Fluor 700–conjugated CD3 (17A2; eBioscience). Cell viability was determined with 7 aminoactinomycin D (Invitrogen) and FITC-conjugated anti–Annexin V. When staining using Annexin V, Annexin V binding buffer (BD) was used. For FACS sorting, splenocytes were stained with PE-conjugated anti-CD4 and FITC-conjugated anti-B220 as described above, and the negatively selected populations were harvested for the adoptive cell transfers. The following antibodies were used for intracytoplasmic staining of lymphocytes: PerCP-conjugated anti-tbet (eBio4B10; eBioscience), FITC-conjugated Bcl-2 (3F11), and Dylight-conjugated anti-Blimp (3H2-E8). Anti-Bim (clone 3C5; a gift from A. Strasser, Walter and Eliza Hall Institute of Medical Research, Parkville, Victoria, Australia) was conjugated to Alexa Fluor 647 using a Protein Labeling kit (A20173; Invitrogen).

CFSE proliferation. Splenic WT and *pri/pri* OT-I T cells were isolated using a MACS column negative selection kit (Miltenyi Biotech) according to the manufacturer's protocol. Naive CD8 T cells were labeled with a final concentration of 5 μM CFSE as per Quah et al. (2007). Bone marrow–derived DCs were derived as described previously (Oliaro et al., 2010) and seeded into 8-well chamber slides at 3×10^4 cells/well. They were then pulsed with SIINFEKL peptide for 1 h and washed twice before the addition of 2×10^4 CFSE-labeled T cells/well. Cells were harvested at the indicated time points.

Immunofluorescence and confocal microscopy. For immunofluorescence staining, 2×10^4 naive splenic WT and *pri/pri* OT-I T cells/well were co-cultured with 3×10^4 SIINFEKL-pulsed bone marrow–derived DCs/well in chamber slides (Oliaro et al., 2010). The cell conjugates formed were fixed at 1 h after incubation with fixative solution (100 mM Pipes, 5 mM $MgSO_4$, 10 mM EGTA, 2 mM DTT, and 3.7% [wt/vol] paraformaldehyde, pH 7.0) for 10 min. The cells were then washed twice and incubated in permeabilization solution (PBS, 0.1% Triton X-100, and 0.5% BSA [wt/vol]) for 5 min before being washed and kept in blocking agent (PBS and 1% BSA [wt/vol]) overnight at 4°C. Primary antibodies against the proteins of interest (anti–LFA-1 [BD], anti–PKC-θ [Santa Cruz Biotechnology, Inc.], and rhodamine-conjugated actin/phalloidin [Invitrogen]), together with mouse α-tubulin (Rocklands) or rabbit α-tubulin (Sigma-Aldrich), were added and incubated for 45 min at 4°C in the dark. Secondary antibodies (anti–rat and anti–rabbit Alexa Fluor 488 and anti–mouse and anti–rabbit Alexa Fluor 546) were added after washing and incubated for another 45 min at 4°C in the dark. The cells were then washed and mounted in ProLong Gold antifade reagent with DAPI (Invitrogen). Cells were imaged using a confocal microscope (Fluoview FV1000; Olympus) equipped with a 12.9-mW 488-nm multi-ion argon laser, a 1-mW 543-nm multi-ion green HeNe laser, and an 11-mW 633-nm red HeNe laser. All images were captured using a PlanApoN 60× oil immersion objective (NA = 1.42). The images were subsequently processed using the Olympus Micro FV10-ASW program and displayed as z-stack projections (sections = 0.5 μm). To acquire images in which an immune synapse was formed, conjugates with the MTOC (as marked by α-tubulin) of T cells polarized to the interface with the DCs were chosen. Blinded scoring of the images was used as a means for quantifying the localization of proteins of interest. An integer score was given from 3 (very polarized to the DC–T cell interface), to 0 (not polarized), to −3 (very polarized away from the interface).

Chromium release killing assay. Splenocytes from C57BL/6 mice were pulsed with 1 μM SIINFEKL peptide for 2 h at room temperature before irradiation at 6 Gy for 30 min. Splenocytes from WT or *pri/pri* OT-I mice were added to the irradiated C57BL/6 splenocytes with the addition of 50 U/ml IL-2 and cultured for 5 d. DCs labeled with 100 μCi Cr^{51} were pulsed with SIINFEKL peptide for 1 h at 37°C. Activated WT and *pri/pri* OT-I splenocytes were added to the DCs at the indicated ratios and incubated at 37°C for 4 h. Supernatant was collected and analyzed for chromium release by an automatic gamma counter (Wallac Wizard 1470; PerkinElmer).

T cell stimulation. Spleen cells from control and mutant mice were isolated, red cells were lysed, and the cells were counted by trypan blue exclusion. Three million cells (per milliliter in a 24-well plate) from each animal were cultured in the presence or absence of 25 ng/ml IL-7 (R&D Systems) with the complete tissue culture medium at 37°C and 5% CO_2 for the indicated time points. Cells were stained as in Flow cytometry of murine cells.

Human samples. Peripheral blood was collected from normal healthy donors (Australian Red Cross Blood Service) and DOCK8-deficient patients (Table I). All human experiments were approved by the Sydney South West Area Health Service and St. Vincent's Hospital Darlinghurst Human Research Ethics Committees, as well as by the institutional review boards of the Necker Medical School, the Rockefeller University, and the National Institute of Allergy and Infectious Diseases (National Institutes of Health). For analysis, the following mAbs were used: FITC-conjugated anti–human CCR7 (150503; R&D systems), PerCP-Cy5.5–conjugated anti–human CD45RA (HI100; eBioscience), PE-Cy7–conjugated anti-CD4 (SK3; BD), Pacific blue–conjugated anti–human CD8 (RPA-T8; BD), eFluor450-conjugated anti–human CD127 (eBioRDR5; eBioscience), PE-conjugated anti–human CD244 (2B4; Beckman Coulter, c1.7), PE-conjugated anti–human CD57 (HCD57; BioLegend), APC-human–conjugated anti-CX3CR1

(2A9-1; BioLegend), APC-conjugated anti–human CD27 (O323; eBioscience), PE-conjugated anti–human CD95 (DX2; BD), APC-conjugated anti–human CD11a (HI111; BD), PE-conjugated anti–human CD11b (D12; BD), APC-conjugated anti–human CD28 (CD28.2; BioLegend), PE-conjugated anti–human perforin (dG9; eBioscience), and APC-conjugated anti–human Granzyme B (GB11; Invitrogen). CD4 and CD8 T cells were isolated from freeze thawed PBMCs using Dynal beads (Invitrogen) as per the manufacturer's instructions. $CD4^+$ T cells were labeled with anti-CCR7 and anti-CD45RA mAbs and then sorted into naive and memory populations using a FACSAria (BD). Naive and memory CD4 T cells were isolated as $CD45RA^+CCR7^+$ and $CD45RA^-CCR7^{+/-}$ cells, respectively, whereas naive and different central and effector memory CD8 T cells were isolated by sorting $CD45RA^+CCR7^+$, $CD45RA^-CCR7^{-/+}$, and $CD45RA^+CCR7^-$ cells. CD4 and CD8 naive and memory T cell subsets were labeled with CFSE and cultured with TAE beads (one bead for every two cells; Miltenyi Biotech) with or without 20 U/ml recombinant human IL-2 (Millipore) for 5 d. After this time, proliferation was determined by measuring CFSE dilution.

Data analysis and statistics. Statistical analyses were performed using Prism software (GraphPad Software) or Excel (Microsoft). Statistical comparison was performed with unpaired Student's *t* tests and χ^2 analysis as noted in the text.

Online supplemental material. Fig. S1 shows extended phenotypic analysis of human DOCK8-deficient $CD8^+$ T cells. Fig. S2 shows T cell counts in blood and LNs for *Dock8*$^{pri/pri}$ and C57BL/6. Fig. S3 shows that there is no evidence of an exhausted CD8 T cell phenotype in *Dock8*$^{pri/pri}$ and *Dock8*$^{cpm/cpm}$ mice. Fig. S4 compares T cell numbers in *Dock8*$^{pri/pri}$, *Dock8*$^{cpm/cpm}$, and C57BL/6 mice. Fig. S5 shows further analysis of thymic subsets in *Dock8*$^{pri/pri}$ mice. Fig. S6 quantifies CD127 on the surface of T cell subsets from *Dock8*$^{pri/pri}$ and C57BL/6 mice. Fig. S7 shows survival of *Dock8*$^{pri/pri}$ and C57BL/6 T cells in culture with and without the addition of IL-7. Fig. S8 shows a chromium release assay using *Dock8*$^{pri/pri}$ OT-I T cells. Online supplemental material is available at http://www.jem.org/cgi/content/full/jem.20110345/DC1.

We wish to thank D. Howard, H. Burke, and J. Wang (Australian National University [ANU], Canberra, Australian Capital Territory, Australia) for expert technical assistance, the staff at the ANU Bioscience Division for animal husbandry, the Australian Phenomics Facility genotyping and mapping team for genetic analysis, the Garvan Institute Flow Facility for cell sorting, F. Carbone for OT-I mice, S. Turner for recombinant influenza constructs, A. Strasser for Bim antibody, and Dr. H. Su (National Institutes of Health, Bethesda, MD) for genotyping patient #6.

This work was supported by contract U54 AI054523 from the National Institutes of Health (to C.C. Goodnow and E.M. Bertram), The Wellcome Trust (C.C. Goodnow and R.J. Cornall), a National Health and Medical Research Council (NHMRC) Program Grant (to C.C. Goodnow and S.G. Tangye), and an NHMRC Project Grant (to E.M. Bertram). C.C. Goodnow was supported by an Australian Research Council Federation Fellowship and is an NHMRC Australia Fellow. C.S. Ma was supported by a Peter Doherty Research Fellowship and is the recipient of a Career Development Award from the NHMRC. S.G. Tangye is a Senior Research Fellow of the NHMRC, and K.L. Randall was an NHMRC Medical Postgraduate Scholar.

The authors declare that they have no competing financial interests.

Submitted: 14 February 2011
Accepted: 15 September 2011

REFERENCES

Appay, V., R.A.W. van Lier, F. Sallusto, and M. Roederer. 2008. Phenotype and function of human T lymphocyte subsets: consensus and issues. *Cytometry A*. 73:975–983.

Atherton, D.J., A.R. Gennery, and A.J. Cant. 2004. The neonate. *In* Rook's Textbook of Dermatology, Vol. 1. Seventh edition. T. Burns, S. Breathnach, N. Cox, and C. Griffiths, editors. Blackwell Publishing, Carlton, Australia. 14:66–14:67.

Bachmann, M.F., R.R. Beerli, P. Agnellini, P. Wolint, K. Schwarz, and A. Oxenius. 2006. Long-lived memory CD8+ T cells are programmed by prolonged antigen exposure and low levels of cellular activation. *Eur. J. Immunol.* 36:842–854. http://dx.doi.org/10.1002/eji.200535730

Badour, K., J. Zhang, F. Shi, M.K. McGavin, V. Rampersad, L.A. Hardy, D. Field, and K.A. Siminovitch. 2003. The Wiskott-Aldrich syndrome protein acts downstream of CD2 and the CD2AP and PSTPIP1 adaptors to promote formation of the immunological synapse. *Immunity*. 18:141–154. http://dx.doi.org/10.1016/S1074-7613(02)00516-2

Beck, L.A., M. Boguniewicz, T. Hata, L.C. Schneider, J. Hanifin, R. Gallo, A.S. Paller, S. Lieff, J. Reese, D. Zaccaro, et al. 2009. Phenotype of atopic dermatitis subjects with a history of eczema herpeticum. *J. Allergy Clin. Immunol.* 124:260–269. http://dx.doi.org/10.1016/j.jaci.2009.05.020

Bittner, T.C., U. Pannicke, E.D. Renner, G. Notheis, F. Hoffmann, B.H. Belohradsky, U. Wintergerst, M. Hauser, B. Klein, K. Schwarz, et al. 2010. Successful long-term correction of autosomal recessive hyper-IgE syndrome due to DOCK8 deficiency by hematopoietic stem cell transplantation. *Klin. Padiatr.* 222:351–355. http://dx.doi.org/10.1055/s-0030-1265135

Bosticardo, M., F. Marangoni, A. Aiuti, A. Villa, and M. Grazia Roncarolo. 2009. Recent advances in understanding the pathophysiology of Wiskott-Aldrich syndrome. *Blood*. 113:6288–6295. http://dx.doi.org/10.1182/blood-2008-12-115253

Brenchley, J.M., N.J. Karandikar, M.R. Betts, D.R. Ambrozak, B.J. Hill, L.E. Crotty, J.P. Casazza, J. Kuruppu, S.A. Migueles, M. Connors, et al. 2003. Expression of CD57 defines replicative senescence and antigen-induced apoptotic death of CD8+ T cells. *Blood*. 101:2711–2720. http://dx.doi.org/10.1182/blood-2002-07-2103

Cannon, J.L., and J.K. Burkhardt. 2004. Differential roles for Wiskott-Aldrich syndrome protein in immune synapse formation and IL-2 production. *J. Immunol.* 173:1658–1662.

Carlson, C.M., B.T. Endrizzi, J. Wu, X. Ding, M.A. Weinreich, E.R. Walsh, M.A. Wani, J.B. Lingrel, K.A. Hogquist, and S.C. Jameson. 2006. Kruppel-like factor 2 regulates thymocyte and T-cell migration. *Nature*. 442:299–302. http://dx.doi.org/10.1038/nature04882

Casanova, J.-L., and L. Abel. 2007. Primary immunodeficiencies: a field in its infancy. *Science*. 317:617–619. http://dx.doi.org/10.1126/science.1142963

Cerundolo, V., and H. de la Salle. 2006. Description of HLA class I- and CD8-deficient patients: Insights into the function of cytotoxic T lymphocytes and NK cells in host defense. *Semin. Immunol.* 18:330–336. http://dx.doi.org/10.1016/j.smim.2006.07.006

Champagne, P., G.S. Ogg, A.S. King, C. Knabenhans, K. Ellefsen, M. Nobile, V. Appay, G.P. Rizzardi, S. Fleury, M. Lipp, et al. 2001. Skewed maturation of memory HIV-specific CD8 T lymphocytes. *Nature*. 410:106–111. http://dx.doi.org/10.1038/35065118

Chen, G., P. Shankar, C. Lange, H. Valdez, P.R. Skolnik, L. Wu, N. Manjunath, and J. Lieberman. 2001. CD8 T cells specific for human immunodeficiency virus, Epstein-Barr virus, and cytomegalovirus lack molecules for homing to lymphoid sites of infection. *Blood*. 98:156–164. http://dx.doi.org/10.1182/blood.V98.1.156

Côté, J.-F., and K. Vuori. 2007. GEF what? Dock180 and related proteins help Rac to polarize cells in new ways. *Trends Cell Biol.* 17:383–393. http://dx.doi.org/10.1016/j.tcb.2007.05.001

de Beaucoudrey, L., A. Puel, O. Filipe-Santos, A. Cobat, P. Ghandil, M. Chrabieh, J. Feinberg, H. von Bernuth, A. Samarina, L. Jannière, et al. 2008. Mutations in *STAT3* and *IL12RB1* impair the development of human IL-17–producing T cells. *J. Exp. Med.* 205:1543–1550. http://dx.doi.org/10.1084/jem.20080321

de la Calle-Martin, O., M. Hernandez, J. Ordi, N. Casamitjana, J.I. Arostegui, I. Caragol, M. Ferrando, M. Labrador, J.L. Rodriguez-Sanchez, and T. Espanol. 2001. Familial CD8 deficiency due to a mutation in the CD8 alpha gene. *J. Clin. Invest.* 108:117–123.

de la Salle, H., J. Zimmer, D. Fricker, C. Angenieux, J.P. Cazenave, M. Okubo, H. Maeda, A. Plebani, M.M. Tongio, A. Dormoy, and D. Hanau. 1999. HLA class I deficiencies due to mutations in subunit 1 of the peptide transporter TAP1. *J. Clin. Invest.* 103:R9–R13. http://dx.doi.org/10.1172/JCI5687

Doherty, P.C. 1996. Cytotoxic T cell effector and memory function in viral immunity. *Curr. Top. Microbiol. Immunol.* 206:1–14.

Dunne, P.J., J.M. Faint, N.H. Gudgeon, J.M. Fletcher, F.J. Plunkett, M.V. Soares, A.D. Hislop, N.E. Annels, A.B. Rickinson, M. Salmon, and A.N. Akbar. 2002. Epstein-Barr virus-specific CD8(+) T cells that re-express CD45RA are apoptosis-resistant memory cells that retain replicative potential. *Blood*. 100:933–940. http://dx.doi.org/10.1182/blood-2002-01-0160

Dupré, L., A. Aiuti, S. Trifari, S. Martino, P. Saracco, C. Bordignon, and M.G. Roncarolo. 2002. Wiskott-Aldrich syndrome protein regulates lipid raft dynamics during immunological synapse formation. *Immunity*. 17:157–166. http://dx.doi.org/10.1016/S1074-7613(02)00360-6

Engelhardt, K.R., S. McGhee, S. Winkler, A. Sassi, C. Woellner, G. Lopez-Herrera, A. Chen, H.S. Kim, M.G. Lloret, I. Schulze, et al. 2009. Large deletions and point mutations involving the dedicator of cytokinesis 8 (DOCK8) in the autosomal-recessive form of hyper-IgE syndrome. *J. Allergy Clin. Immunol.* 124:1289–1302. http://dx.doi.org/10.1016/j.jaci.2009.10.038

Gadola, S.D., H.T. Moins-Teisserenc, J. Trowsdale, W.L. Gross, and V. Cerundolo. 2000. TAP deficiency syndrome. *Clin. Exp. Immunol.* 121:173–178. http://dx.doi.org/10.1046/j.1365-2249.2000.01264.x

Gatz, S.A., U. Benninghoff, C. Schütz, A. Schulz, M. Hönig, U. Pannicke, K.H. Holzmann, K. Schwarz, and W. Friedrich. 2011. Curative treatment of autosomal-recessive hyper-IgE syndrome by hematopoietic cell transplantation. *Bone Marrow Transplant.* 46:552–556. http://dx.doi.org/10.1038/bmt.2010.169

Geginat, J., A. Lanzavecchia, and F. Sallusto. 2003. Proliferation and differentiation potential of human CD8+ memory T-cell subsets in response to antigen or homeostatic cytokines. *Blood*. 101:4260–4266. http://dx.doi.org/10.1182/blood-2002-11-3577

Hamann, D., S. Kostense, K.C. Wolthers, S.A. Otto, P.A. Baars, F. Miedema, and R.A. van Lier. 1999. Evidence that human $CD8^+CD45RA^+CD27^-$ cells are induced by antigen and evolve through extensive rounds of division. *Int. Immunol.* 11:1027–1033. http://dx.doi.org/10.1093/intimm/11.7.1027

Harty, J.T., A.R. Tvinnereim, and D.W. White. 2000. CD8+ T cell effector mechanisms in resistance to infection. *Annu. Rev. Immunol.* 18:275–308. http://dx.doi.org/10.1146/annurev.immunol.18.1.275

Hogquist, K.A., S.C. Jameson, W.R. Heath, J.L. Howard, M.J. Bevan, and F.R. Carbone. 1994. T cell receptor antagonist peptides induce positive selection. *Cell*. 76:17–27. http://dx.doi.org/10.1016/0092-8674(94)90169-4

Intlekofer, A.M., E.J. Wherry, and S.L. Reiner. 2006. Not-so-great expectations: re-assessing the essence of T-cell memory. *Immunol. Rev.* 211:203–213. http://dx.doi.org/10.1111/j.0105-2896.2006.00396.x

Jenkins, M.R., R. Webby, P.C. Doherty, and S.J. Turner. 2006. Addition of a prominent epitope affects influenza A virus-specific CD8+ T cell immunodominance hierarchies when antigen is limiting. *J. Immunol.* 177:2917–2925.

Kaech, S.M., and R. Ahmed. 2001. Memory CD8+ T cell differentiation: initial antigen encounter triggers a developmental program in naïve cells. *Nat. Immunol.* 2:415–422.

Laffort, C., F. Le Deist, M. Favre, S. Caillat-Zucman, I. Radford-Weiss, M. Debré, S. Fraitag, S. Blanche, M. Cavazzana-Calvo, G. de Saint Basile, et al. 2004. Severe cutaneous papillomavirus disease after haemopoietic stem-cell transplantation in patients with severe combined immune deficiency caused by common gammac cytokine receptor subunit or JAK-3 deficiency. *Lancet*. 363:2051–2054. http://dx.doi.org/10.1016/S0140-6736(04)16457-X

Lazarczyk, M., C. Pons, J.-A. Mendoza, P. Cassonnet, Y. Jacob, and M. Favre. 2008. Regulation of cellular zinc balance as a potential mechanism of EVER-mediated protection against pathogenesis by cutaneous oncogenic human papillomaviruses. *J. Exp. Med.* 205:35–42. http://dx.doi.org/10.1084/jem.20071311

Ma, C.S., G.Y. Chew, N. Simpson, A. Priyadarshi, M. Wong, B. Grimbacher, D.A. Fulcher, S.G. Tangye, and M.C. Cook. 2008. Deficiency of Th17 cells in hyper IgE syndrome due to mutations in *STAT3*. *J. Exp. Med.* 205:1551–1557. http://dx.doi.org/10.1084/jem.20080218

Masopust, D., V. Vezys, E.J. Wherry, and R. Ahmed. 2007. A brief history of CD8 T cells. *Eur. J. Immunol.* 37:S103–S110. http://dx.doi.org/10.1002/eji.200737584

Matloubian, M., C.G. Lo, G. Cinamon, M.J. Lesneski, Y. Xu, V. Brinkmann, M.L. Allende, R.L. Proia, and J.G. Cyster. 2004. Lymphocyte egress from thymus and peripheral lymphoid organs is dependent on S1P receptor 1. *Nature*. 427:355–360. http://dx.doi.org/10.1038/nature02284

Mercado, R., S. Vijh, S.E. Allen, K. Kerksiek, I.M. Pilip, and E.G. Pamer. 2000. Early programming of T cell populations responding to bacterial infection. *J. Immunol.* 165:6833–6839.

Milner, J.D., J.M. Brenchley, A. Laurence, A.F. Freeman, B.J. Hill, K.M. Elias, Y. Kanno, C. Spalding, H.Z. Elloumi, M.L. Paulson, et al. 2008. Impaired T(H)17 cell differentiation in subjects with autosomal dominant hyper-IgE syndrome. *Nature*. 452:773–776. http://dx.doi.org/10.1038/nature06764

Notarangelo, L.D., A. Fischer, R.S. Geha, J.-L. Casanova, H. Chapel, M.E. Conley, C. Cunningham-Rundles, A. Etzioni, L. Hammartröm, S. Nonoyama, et al. 2009. Primary immunodeficiencies: 2009 update. *J. Allergy Clin. Immunol.* 124:1161–1178. http://dx.doi.org/10.1016/j.jaci.2009.10.013

Oliaro, J., V. Van Ham, F. Sacirbegovic, A. Pasam, Z. Bomzon, K. Pham, M.J. Ludford-Menting, N.J. Waterhouse, M. Bots, E.D. Hawkins, et al. 2010. Asymmetric cell division of T cells upon antigen presentation uses multiple conserved mechanisms. *J. Immunol.* 185:367–375. http://dx.doi.org/10.4049/jimmunol.0903627

Papagno, L., C.A. Spina, A. Marchant, M. Salio, N. Rufer, S. Little, T. Dong, G. Chesney, A. Waters, P. Easterbrook, et al. 2004. Immune activation and CD8+ T-cell differentiation towards senescence in HIV-1 infection. *PLoS Biol.* 2:E20. http://dx.doi.org/10.1371/journal.pbio.0020020

Plunkett, F.J., O. Franzese, L.L. Belaramani, J.M. Fletcher, K.C. Gilmour, R. Sharifi, N. Khan, A.D. Hislop, A. Cara, M. Salmon, et al. 2005. The impact of telomere erosion on memory CD8+ T cells in patients with X-linked lymphoproliferative syndrome. *Mech. Ageing Dev.* 126:855–865. http://dx.doi.org/10.1016/j.mad.2005.03.006

Pulecio, J., E. Tagliani, A. Scholer, F. Prete, L. Fetler, O.R. Burrone, and F. Benvenuti. 2008. Expression of Wiskott-Aldrich syndrome protein in dendritic cells regulates synapse formation and activation of naive CD8+ T cells. *J. Immunol.* 181:1135–1142.

Quah, B.J., H.S. Warren, and C.R. Parish. 2007. Monitoring lymphocyte proliferation in vitro and in vivo with the intracellular fluorescent dye carboxyfluorescein diacetate succinimidyl ester. *Nat. Protoc.* 2:2049–2056. http://dx.doi.org/10.1038/nprot.2007.296

Ramoz, N., L.-A. Rueda, B. Bouadjar, L.-S. Montoya, G. Orth, and M. Favre. 2002. Mutations in two adjacent novel genes are associated with epidermodysplasia verruciformis. *Nat. Genet.* 32:579–581. http://dx.doi.org/10.1038/ng1044

Randall, K.L., T. Lambe, A.L. Johnson, B. Treanor, E. Kucharska, H. Domaschenz, B. Whittle, L.E. Tze, A. Enders, T.L. Crockford, et al. 2009. Dock8 mutations cripple B cell immunological synapses, germinal centers and long-lived antibody production. *Nat. Immunol.* 10:1283–1291. http://dx.doi.org/10.1038/ni.1820

Renner, E.D., S. Rylaarsdam, S. Anover-Sombke, A.L. Rack, J. Reichenbach, J.C. Carey, Q. Zhu, A.F. Jansson, J. Barboza, L.F. Schimke, et al. 2008. Novel signal transducer and activator of transcription 3 (STAT3) mutations, reduced T(H)17 cell numbers, and variably defective STAT3 phosphorylation in hyper-IgE syndrome. *J. Allergy Clin. Immunol.* 122:181–187. http://dx.doi.org/10.1016/j.jaci.2008.04.037

Romero, P., A. Zippelius, I. Kurth, M.J. Pittet, C. Touvrey, E.M. Iancu, P. Corthesy, E. Devevre, D.E. Speiser, and N. Rufer. 2007. Four functionally distinct populations of human effector-memory CD8+ T lymphocytes. *J. Immunol.* 178:4112–4119.

Rufer, N., A. Zippelius, P. Batard, M.J. Pittet, I. Kurth, P. Corthesy, J.C. Cerottini, S. Leyvraz, E. Roosnek, M. Nabholz, and P. Romero. 2003. Ex vivo characterization of human CD8+ T subsets with distinct replicative history and partial effector functions. *Blood*. 102:1779–1787. http://dx.doi.org/10.1182/blood-2003-02-0420

Sallusto, F., A. Lanzavecchia, K. Araki, and R. Ahmed. 2010. From vaccines to memory and back. *Immunity*. 33:451–463. http://dx.doi.org/10.1016/j.immuni.2010.10.008

Published October 17, 2011

Scholer, A., S. Hugues, A. Boissonnas, L. Fetler, and S. Amigorena. 2008. Intercellular adhesion molecule-1-dependent stable interactions between T cells and dendritic cells determine CD8+ T cell memory. *Immunity*. 28:258–270. http://dx.doi.org/10.1016/j.immuni.2007.12.016

Shiow, L.R., D.W. Roadcap, K. Paris, S.R. Watson, I.L. Grigorova, T. Lebet, J. An, Y. Xu, C.N. Jenne, N. Föger, et al. 2008. The actin regulator coronin 1A is mutant in a thymic egress-deficient mouse strain and in a patient with severe combined immunodeficiency. *Nat. Immunol.* 9:1307–1315. http://dx.doi.org/10.1038/ni.1662

Surh, C.D., and J. Sprent. 2008. Homeostasis of naive and memory T cells. *Immunity*. 29:848–862. http://dx.doi.org/10.1016/j.immuni.2008.11.002

Teixeiro, E., M.A. Daniels, S.E. Hamilton, A.G. Schrum, R. Bragado, S.C. Jameson, and E. Palmer. 2009. Different T cell receptor signals determine CD8+ memory versus effector development. *Science*. 323:502–505. http://dx.doi.org/10.1126/science.1163612

van Stipdonk, M.J., E.E. Lemmens, and S.P. Schoenberger. 2001. Naïve CTLs require a single brief period of antigenic stimulation for clonal expansion and differentiation. *Nat. Immunol.* 2:423–429.

Walter, E.A., P.D. Greenberg, M.J. Gilbert, R.J. Finch, K.S. Watanabe, E.D. Thomas, and S.R. Riddell. 1995. Reconstitution of cellular immunity against cytomegalovirus in recipients of allogeneic bone marrow by transfer of T-cell clones from the donor. *N. Engl. J. Med.* 333:1038–1044. http://dx.doi.org/10.1056/NEJM199510193331603

Williams, M.A., B.J. Holmes, J.C. Sun, and M.J. Bevan. 2006a. Developing and maintaining protective CD8+ memory T cells. *Immunol. Rev.* 211:146–153. http://dx.doi.org/10.1111/j.0105-2896.2006.00389.x

Williams, M.A., A.J. Tyznik, and M.J. Bevan. 2006b. Interleukin-2 signals during priming are required for secondary expansion of CD8+ memory T cells. *Nature*. 441:890–893. http://dx.doi.org/10.1038/nature04790

Wollenberg, A., S. Wetzel, W.H.C. Burgdorf, and J. Haas. 2003. Viral infections in atopic dermatitis: pathogenic aspects and clinical management. *J. Allergy Clin. Immunol.* 112:667–674. http://dx.doi.org/10.1016/j.jaci.2003.07.001

Zhang, Q., J.C. Davis, I.T. Lamborn, A.F. Freeman, H. Jing, A.J. Favreau, H.F. Matthews, J. Davis, M.L. Turner, G. Uzel, et al. 2009. Combined immunodeficiency associated with DOCK8 mutations. *N. Engl. J. Med.* 361:2046–2055. http://dx.doi.org/10.1056/NEJMoa0905506

Published October 17, 2011

JEM

SUPPLEMENTAL MATERIAL

Randall et al., http://www.jem.org/cgi/content/full/jem.20110345/DC1

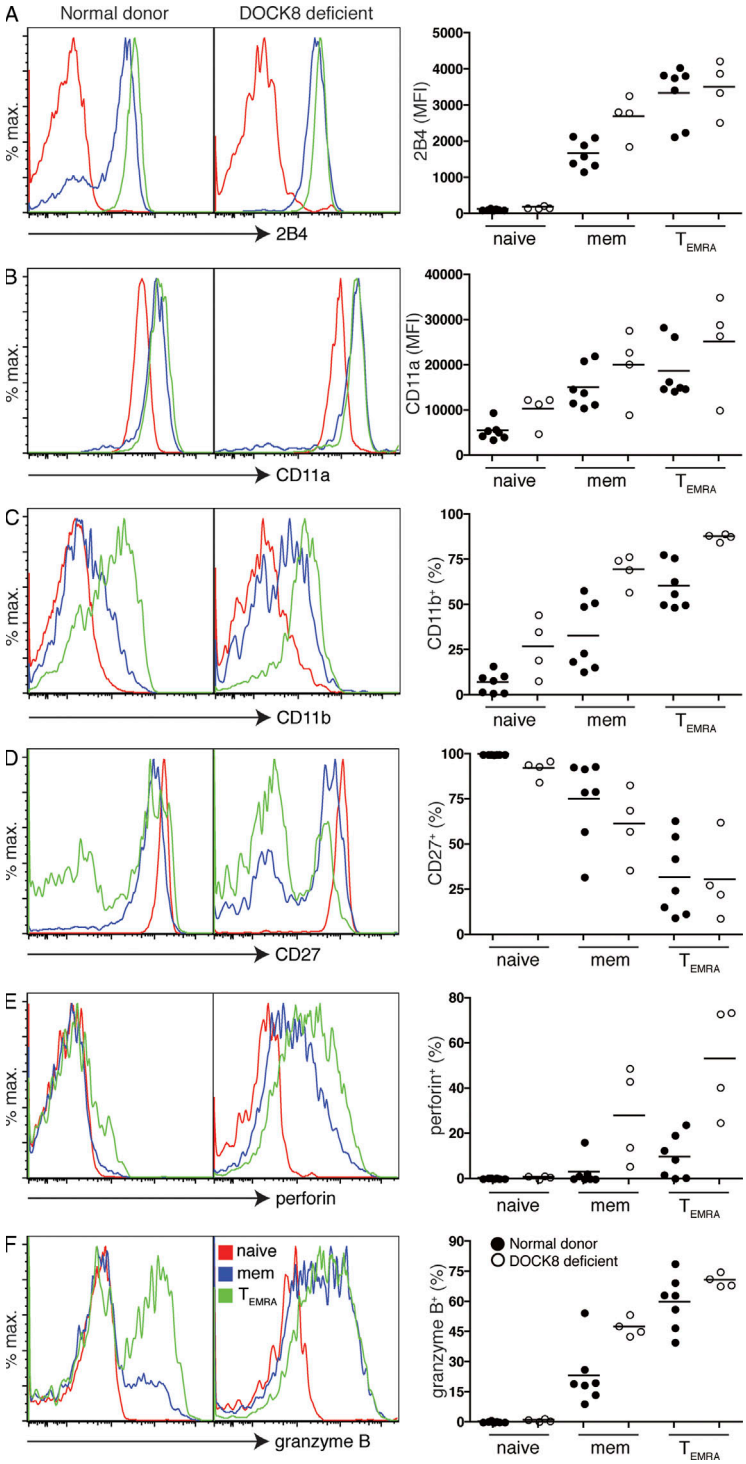

Figure S1. Extended phenotypic analysis of human DOCK8-deficient CD8⁺ T cells. (A–G) PBMCs from normal donors (n = 7) or DOCK8-deficient patients (n = 4) were labeled with anti-CD8, anti-CD45RA, and anti-CCR7 mAbs and either isotype control or mAb specific for CD27, CD244 (2B4), CD11a, or CD11b. The expression of these molecules on naive ($CD45RA^+CCR7^+$), memory ($CD45RA^-CCR7^-$), and T_{EMRA} ($CD45RA^+CCR7^-$) subsets of CD8 T cells was then determined. Perforin and granzyme B expression were also assessed after fixing and permeabilizing the cells after labeling with anti-CD8, anti-CD45RA, and anti-CCR7 mAbs. The histogram plots are from one representative normal donor or control. Each value in the graphs corresponds to an individual normal donor or patient; horizontal bars represent the mean. MFI, mean fluorescence intensity.

Published October 17, 2011

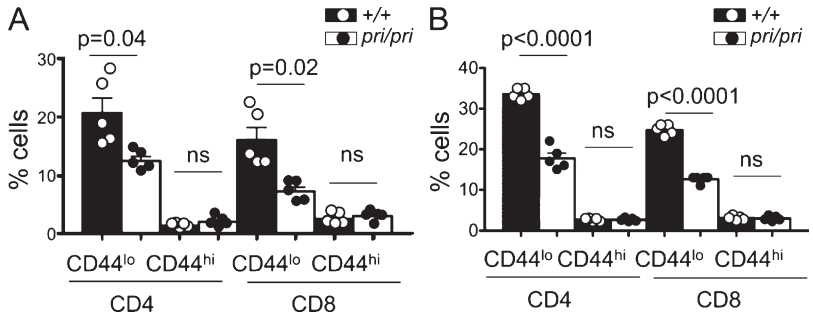

Figure S2. Quantitation of T cells in blood and LNs. (A and B) Quantitation of T cells in blood (A) and LNs (B) for age-matched C57BL/6 and *Dock-8*$^{pri/pri}$ mice. Data are representative of at least three independent experiments. Bars are means, error bars indicate SEM, and dots indicate individual mice. Statistical analysis was performed by the unpaired Student's *t* test with Welch's correction.

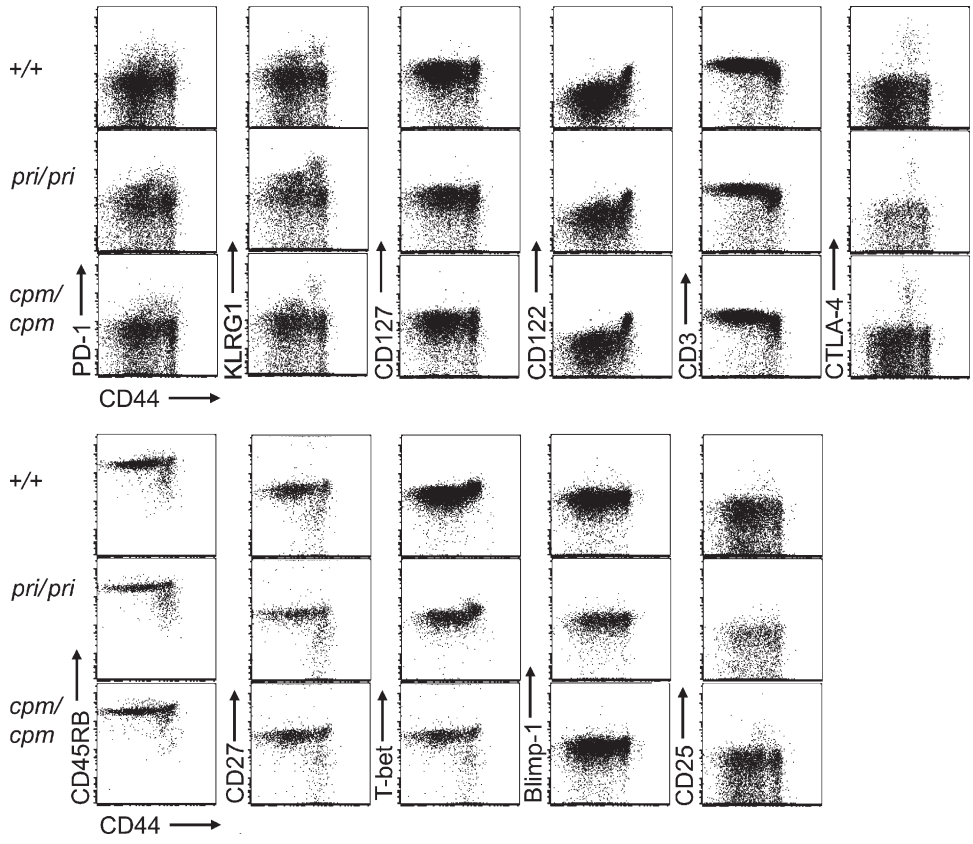

Figure S3. Extended phenotype analysis of CD8 T cells in *Dock8*$^{pri/pri}$ and *Dock8*$^{cpm/cpm}$ mice. Representative flow cytometry plots of surface marker staining of CD8 cells from WT, primurus (*pri/pri*), and captain morgan (*cpm/cpm*) mice.

Published October 17, 2011

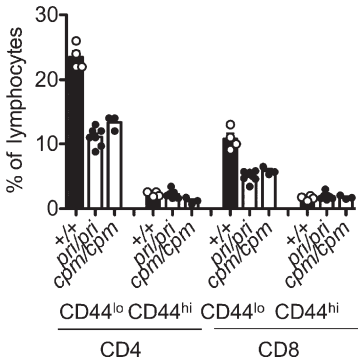

Figure S4. Quantitation of T cells in *Dock8*$^{pri/pri}$ and *Dock8*$^{cpm/cpm}$ mice. Quantitation of splenic T cells of C57BL/6, *Dock8*$^{pri/pri}$, and *Dock8*$^{cpm/cpm}$ mice. Data are representative of at least two independent experiments. Bars are means, error bars indicate SEM, and dots indicate individual mice

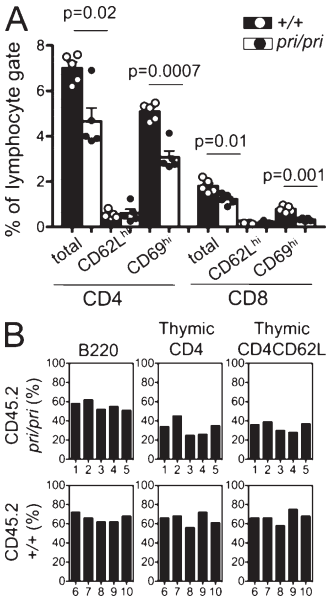

Figure S5. Further analysis of thymic subsets in *Dock8*$^{pri/pri}$ mice. (A) Analysis of thymic subsets in WT and *Dock8*$^{pri/pri}$ mice. In most cases, the number of CD4 and CD8 cells did not vary significantly between WT and mutant mice, but this was variable, and in some mice there were decreased numbers of CD4 and CD8 cells in the thymus of *Dock8*$^{pri/pri}$ mice as shown here. Bars are means, dots indicate individual mice, and error bars indicate SEM. (B) Figure shows reconstitution of various cellular subsets in 50:50 bone marrow chimeras with the proportion in each mouse indicated by each bar (individual mouse numbers on x axis).

Published October 17, 2011

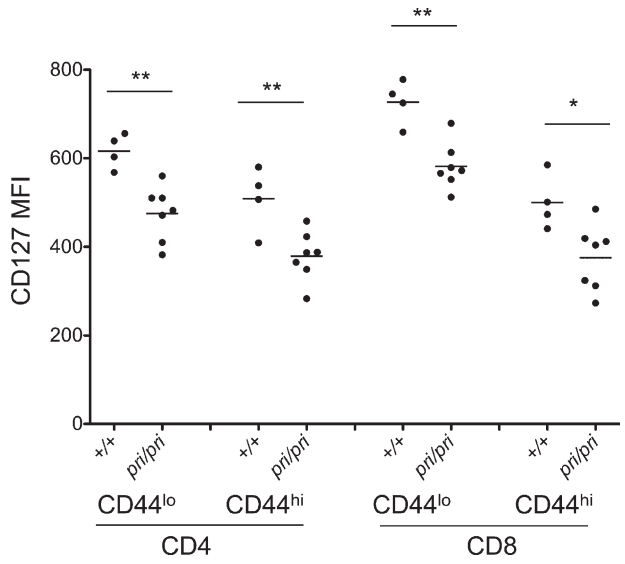

Figure S6. Expression of CD127. Expression of CD127 on splenic T cells of C57BL/6 and *Dock8*$^{pri/pri}$ mice. Data are representative of two independent experiments. Statistical analysis was performed using the unpaired Student's *t* test (*, P <0.05; **, P <0.005). Horizontal bars show arithmetic mean. MFI, mean fluorescence intensity.

Published October 17, 2011

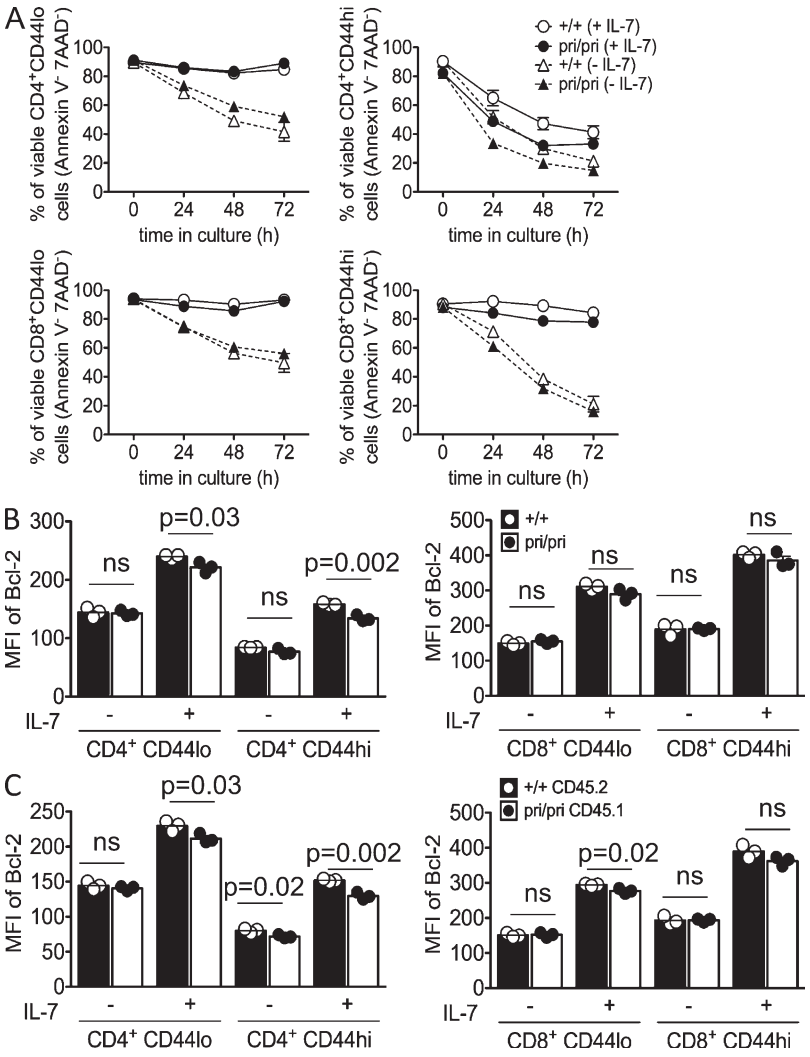

Figure S7. Survival of *Dock8*$^{pri/pri}$ T cells in culture with or without IL-7. (A) Equal numbers of freshly isolated spleen cells cultured in the presence (25 ng/ml) and absence of IL-7. Graphs show survival curves for T cell subsets in the presence and absence of IL-7 for the indicated time points for WT (open symbols) and *Dock8*$^{pri/pri}$ (closed symbols). (B and C) Equal numbers of freshly isolated spleen cells were cultured (B) and co-cultured (C) in the presence (25 ng/ml) and absence of IL-7 for 48 h. Cells were then collected, stained, and analyzed on flow cytometry for induction of Bcl-2 for WT (open circles, closed bars) and *Dock8*$^{pri/pri}$ (closed circles, open bars). MFI, mean fluorescence intensity.

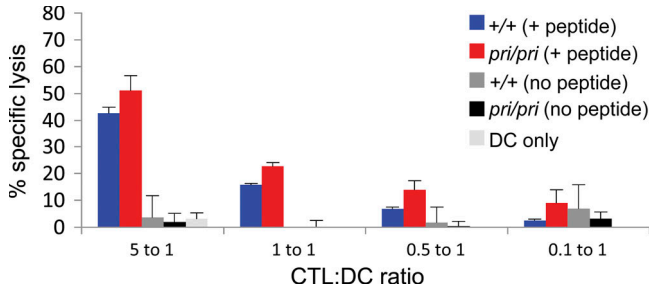

Figure S8. Cytotoxicity of *pri/pri* OT-I T cells. Splenocytes from C57BL/6 mice were pulsed with 1 µM SIINFEKL peptide for 2 h at room temperature before irradiation at 6 Gy for 30 min. Splenocytes from WT or *pri/pri* OT-I mice were added to the irradiated C57BL/6 splenocytes with the addition of 50 U/ml IL-2 and cultured for 5 d. DCs labeled with 100 µCi Cr^{51} were pulsed with SIINFEKL peptide for 1 h at 37°C. Activated WT (blue) and *pri/pri* OT-I (red) splenocytes were added to the DCs at the indicated ratios and incubated at 37°C for 4 h. Supernatant was collected and analyzed for chromium release by a Wallac Wizard 1470 automatic gamma counter. Bars are means, and error bars indicate SD.